

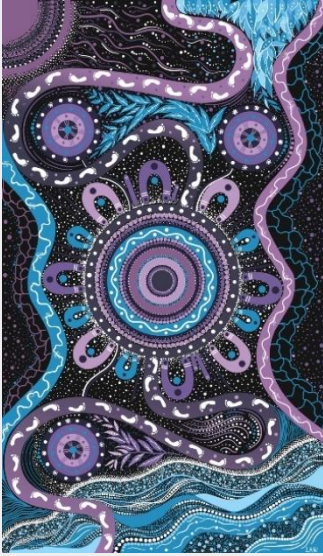
# Validation of dynamic models for distributed PV and composite load

June 2025

Benchmarking of DERAEMO1 and  
CMLD models in PSS®E against  
disturbances:

13<sup>th</sup> February 2024, 25<sup>th</sup> March 2024, 27<sup>th</sup> March 2024





**We acknowledge the Traditional Custodians of the land, seas and waters across Australia. We honour the wisdom of Aboriginal and Torres Strait Islander Elders past and present and embrace future generations.**

**We acknowledge that, wherever we work, we do so on Aboriginal and Torres Strait Islander lands. We pay respect to the world's oldest continuing culture and First Nations peoples' deep and continuing connection to Country; and hope that our work can benefit both people and Country.**

'Journey of unity: AEMO's Reconciliation Path' by Lani Balzan

AEMO Group is proud to have launched its first [Reconciliation Action Plan](#) in May 2024. 'Journey of unity: AEMO's Reconciliation Path' was created by Wiradjuri artist Lani Balzan to visually narrate our ongoing journey towards reconciliation - a collaborative endeavour that honours First Nations cultures, fosters mutual understanding, and paves the way for a brighter, more inclusive future.

## Important notice

### Purpose

This report validates the performance of AEMO's Composite Load (CMLD) and Distributed PV (DPV) models by comparison to measurements during power system events on 13 February 2024, 25 March 2024 and 27 March 2024. These models may be used where appropriate by AEMO and Transmission Network Service Providers (TNSPs) in assessment of power system limits and security studies.

### Disclaimer

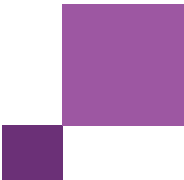
This document or the information in it may be subsequently updated or amended. This document does not constitute legal, business, engineering or technical advice. It should not be relied on as a substitute for obtaining detailed advice about the National Electricity Law, the National Electricity Rules, any other applicable laws, procedures or policies or the capability or performance of relevant equipment. AEMO has made reasonable efforts to ensure the quality of the information in this document but cannot guarantee its accuracy or completeness.

Accordingly, to the maximum extent permitted by law, AEMO and its officers, employees and consultants involved in the preparation of this document:

- make no representation or warranty, express or implied, as to the currency, accuracy, reliability or completeness of the information in this document; and
- are not liable (whether by reason of negligence or otherwise) for any statements or representations in this document, or any omissions from it, or for any use or reliance on the information in it.

### Copyright

© 2025 Australian Energy Market Operator Limited. The material in this publication may be used in accordance with the [copyright permissions on AEMO's website](#).



# Executive summary

Power system models are an essential tool used by AEMO and transmission network service providers (TNSPs) to assess the outcomes of various disturbances and ensure the power system is operated securely within the necessary technical limits. When power system disturbances occur, it is important to test the validity of these models, to ensure they provide an accurate representation of the behaviour of the power system under these conditions.

Three recent power system incidents showed significant relevant behaviours from distributed PV (DPV) and composite load:

- **13 February 2024 (Victoria):** This disturbance was one of the most significant load shake-off events ever observed in the NEM (with more than 1 GW of load shaken-off in Victoria) and represents an important opportunity to validate load models.
- **25 March 2024 and 27 March 2024 (South Australia):** These severe faults in the Adelaide metropolitan area, occurring in periods with high levels of DPV generation, both show clear evidence of an increase in regional operational demand post fault. This provides concrete evidence of the occurrence of DPV shake-off, as predicted by AEMO's earlier analysis. These events provide an important opportunity to validate AEMO's models for both load and DPV, under conditions of high DPV generation.

These three events together provide an important opportunity to test and validate the behaviour of dynamic models that are used to represent composite load and DPV in dynamic power system studies. This report presents testing and validation of AEMO's Composite Load (CMLD) and DPV models in PSS®E against measurements from these three recent events. The development and parameterisation of these models is described in AEMO's previous reports, which remain valid<sup>1</sup>.

Validation against measurements from these three recent events demonstrates that the CMLD+DPV models consistently and significantly outperform ZIP-based models in representing both transient and steady-state conditions.

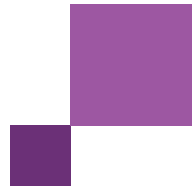
In almost all cases, the CMLD+DPV models provide an improved (and in many cases a significantly improved) representation of DPV and composite load as measured in these disturbances, compared with the traditional ZIP modelling approach.

## Shake-off behaviours

The models provide a reasonable indication of the shake-off behaviours observed from distributed PV and composite load in response to deep voltage disturbances, which cannot be replicated at all by the traditional ZIP

---

<sup>1</sup> AEMO, Managing Distributed energy Resources in Operations, Development Power System Models of DER and load behaviour, <https://aemo.com.au/initiatives/major-programs/nem-distributed-energy-resources-der-program/managing-distributed-energy-resources-in-operations/power-system-model-development>

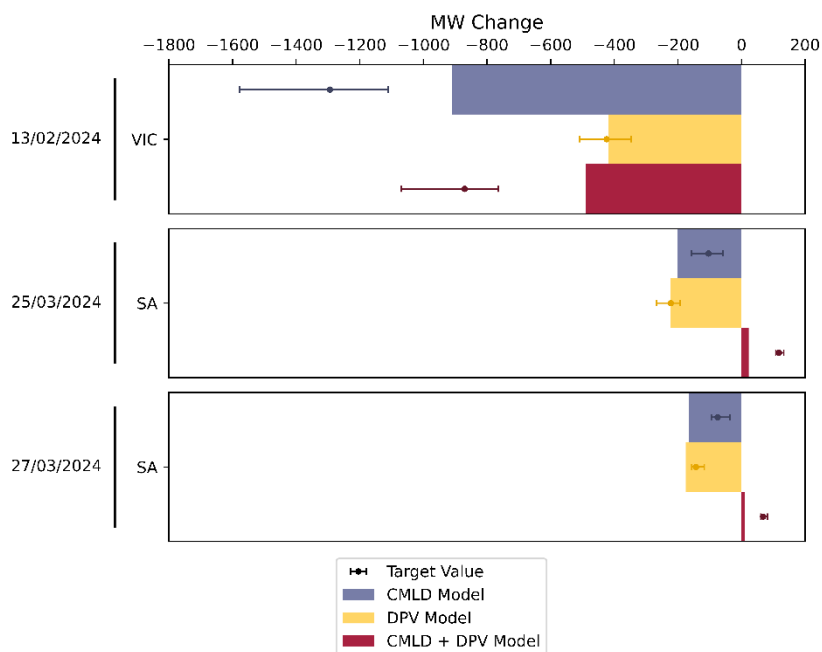


modelling approach. Figure 1 summarises the observed DPV and load shake-off in these three disturbances (“Target value”)<sup>2</sup>, compared with the CMLD and DPV model outcomes:

- The DPV model captures DPV shake-off reasonably accurately in all three cases.
- The CMLD model demonstrates a very considerable amount of load shake-off in the Victorian disturbance but underestimates the full extent of what was observed. The CMLD model overestimates load shake-off in both the South Australian disturbances. This highlights the need for uncertainty margins when applying these models.

Both models provide a considerable improvement over the traditional ZIP model, which does not represent any load or DPV shake-off at all.

**Figure 1 CMLD & DPV model performance across three disturbances**



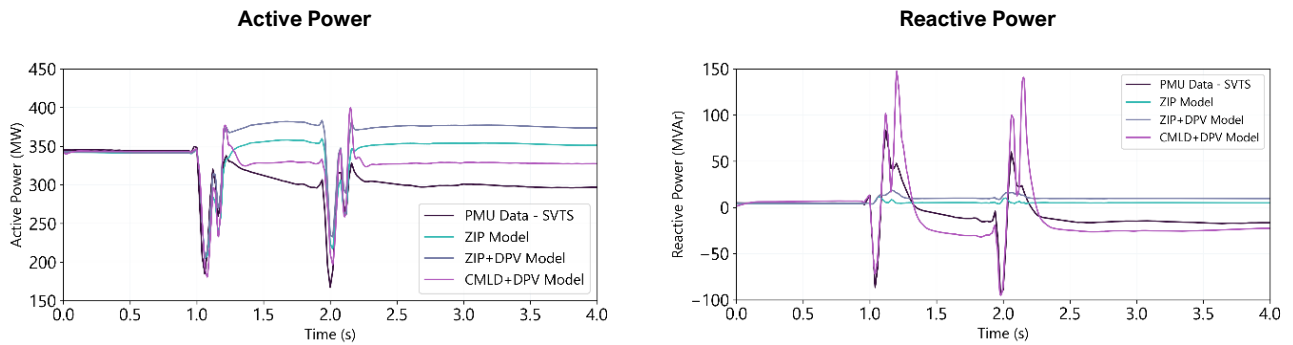
### Transient behaviours

The models also provide a much-improved representation of the transient behaviours of composite load and distributed PV, especially for reactive power.

An example is provided in Figure 2, showing high speed measurements at Springvale Terminal Station compared with model outcomes. The CMLD+DPV model provides a significantly improved representation of the active and reactive power measurements at this location (and the others measured) compared with the traditional ZIP model.

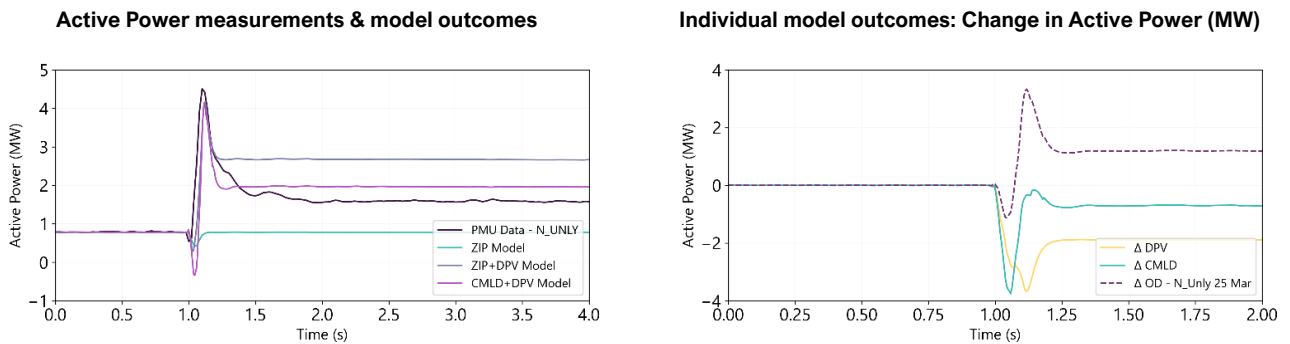
<sup>2</sup> The target values are indicated with dots, with error bars indicating the uncertainty in the actuals estimates.

**Figure 2 PMU data vs playback simulation results: Springvale Terminal Station (SVTS) – 13 February 2024**



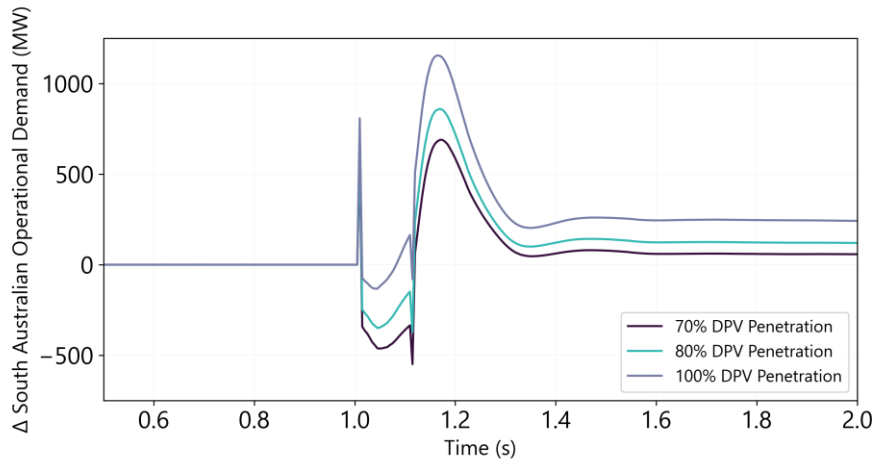
Another example is shown in Figure 3, for the disturbance in South Australia on 25 March 2024, showing measurements at North Unley in the South Australian 11kV network. The data at this location and others consistently shows a significant transient increase or “swing” in operational demand post fault in cases with a high level of DPV operating. This behaviour is observed at radial load feeders supplied by a high proportion of DPV and is consistently replicated well by the CMLD+DPV models. The composite load model (CMLD) recovers post fault slightly faster than the DPV model (shown in the right panel in Figure 3), leading to a significant transient deficit in generation that is much larger than the settling difference related to DPV and load shake-off.

**Figure 3 North Unley – 25 March 2024 – Playback simulation**



When aggregated across a whole region, this behaviour can lead to a significant transient (~200ms duration) increase in regional operational demand post fault. For example, as shown in Figure 4, in South Australia the models suggest the regional demand swing magnitude could exceed ~1000 MW in some projected cases with a more severe fault and higher levels of DPV operating. These effects could have significant impacts on modelling outcomes and power system stability. This highlights the importance of applying accurate models for composite load and DPV, particularly in cases with a significant amount of DPV operating.

Figure 4 Simulation outcomes: 27 March event with more severe credible fault and increasing DPV penetration



### Limitations of the CMLD+DPV models

While the CMLD+DPV models represent a considerable improvement compared with the traditional ZIP model representation, these models have some important limitations. TNSPs and other users should be aware of these limitations and carefully consider if the models are fit for purpose for the specific application.

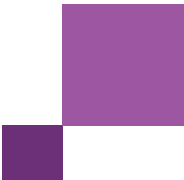
Limitations include:

- **±30% Shake-Off Uncertainty:** The models exhibit uncertainty margins of  $\pm 30\%$  of the contingency size in capturing DPV and load shake-off.
- **Multiple faults:** The models only represent the shake-off associated with the first fault, and then “lock out” any subsequent shake-off that may occur in response to subsequent (potentially deeper) faults. This means it’s important for multi-fault events that the first fault modelled is the most severe (otherwise the models will under-represent the total amount of shake-off).
- **Importance of using both models together:** The studies emphasise the importance of using the CMLD model together with the DPV model. If only the DPV model is used (in conjunction with the traditional ZIP model), the load shake-off will not be captured and the model outcomes can be severely incorrect in some cases.

### Recommendations

AEMO provides the following recommendations:

- **Review of Limit Advice:** TNSPs are urged to revisit their limit advice, ensuring it appropriately accounts for the dynamic behaviours of load and DPV observed during disturbances. Impacts to limits could be related to DPV and load shake-off, and to the significant transient “swing” in operational demand that is observed post fault and can be much larger than the settling shake-off levels. TNSPs retain responsibility for ensuring the models used for any studies are fit-for-purpose.
- **Model Applicability:** Any use of these models must account for their known limitations, and their validity should be confirmed for each specific application. AEMO will continue collaborating with TNSPs to refine and validate the models, especially as they are applied to novel use cases.

- 
- **Data Requirements:** These studies highlight the need for improved datasets for assessing power system behaviours and validation of power system models. This includes improvements to high-speed monitoring, improved DPV fleet data, and improved information on load composition. AEMO will collaborate with stakeholders to progress this.

These actions will help refine model accuracy, increase confidence in the validity of the models, and enhance planning and operation of the power system securely in the context of increasing DPV penetration and evolving network dynamics.

# Contents

Executive summary	3
1 Introduction	11
2 Victoria: 13 February 2024	13
2.1 Event overview	13
2.2 Representation of multiple faults	14
2.3 Radial measurements (Single Load Infinite Bus simulations)	15
2.4 System-wide studies	22
3 South Australia: 25 March 2024	30
3.1 Event overview	30
3.2 Radial measurements (Single Load Infinite Bus simulations)	31
3.3 System-wide studies	34
4 South Australia: 27 March 2024	40
4.1 Event overview	40
4.2 Radial measurements (Single Load Infinite Bus simulations)	41
4.3 System wide studies	43
5 Operational Demand Swings	48
5.1 Influence of DPV levels on operational demand swings	49
5.2 Regional level implications	49
5.3 Impact of fault severity and DPV penetration on operational demand swings	50
6 Summary and recommendations	53
6.1 Summary of findings	53
6.2 Recommendations	55
6.3 Future improvements	56
A1. Glossary	58
A2. Data sources	59

## Tables

Table 1	Event summary – 13 February 2024	13
Table 2	Terminal station summary of voltage sag, DPV participation and end-use load type	16
Table 3	Simulation event summary – 13 February 2024	22
Table 4	Summary of change in demand and distributed PV – 13 February 2024	27
Table 5	Assessment of model performance – 13 February 2024	29

Table 6	Event summary – 25 March 2024	30
Table 7	Terminal station summary of voltage sag, DPV participation and end-use load type	31
Table 8	Simulation event summary – 25 March 2024	35
Table 9	Summary of change in demand and distributed PV – 25 March 2024	38
Table 10	Assessment of model performance – 25 March 2024	39
Table 11	Event summary – 27 March 2024	40
Table 12	Terminal station summary of voltage sag, DPV participation and end-use load type	41
Table 13	Simulation event summary – 27 March 2024	43
Table 14	Summary of change in demand and distributed PV – 27 March 2024	46
Table 15	Assessment of model performance – 27 March 2024	47
Table 16	Operational Demand swings captured from PMU data for 25 March and 27 March events in SA	49
Table 17	Known model limitations and areas for improvement	56
Table 18	Data sources used in this report	59

## Figures

Figure 1	CMLD & DPV model performance across three disturbances	4
Figure 2	PMU data vs playback simulation results: Springvale Terminal Station (SVTS) – 13 February 2024	5
Figure 3	North Unley – 25 March 2024 – Playback simulation	5
Figure 4	Simulation outcomes: 27 March event with more severe credible fault and increasing DPV penetration	6
Figure 5	Map – 13 February 2024	14
Figure 6	Voltage and active power at Richmond Terminal Station (RTS) 220 kV network	15
Figure 7	PMU data vs playback simulation results: Richmond Terminal Station (RTS)	17
Figure 8	Active power response of each model: Richmond Terminal Station (RTS)	18
Figure 9	PMU data vs playback simulation results: West Melbourne Terminal Station (WMTS)	18
Figure 10	Active power response of each model: West Melbourne Terminal Station (WMTS)	19
Figure 11	PMU data vs playback simulation results: Springvale Terminal Station (SVTS)	19
Figure 12	Active power response of each model: Springvale Terminal Station (SVTS)	20
Figure 13	PMU data vs playback simulation results: Ringwood Terminal Station (RWTS)	21
Figure 14	Active power response of each model: Ringwood Terminal Station (RWTS)	22
Figure 15	Voltages – 13 February 2024	23
Figure 16	Active/reactive power – 13 February 2024 – 500kV SMTS to HWTS Feeder	24
Figure 17	Active/reactive power – 13 February 2024 – 500kV MLTS to HGTS Feeder	24
Figure 18	DPV measurements – Victoria total – 13 February 2024	25

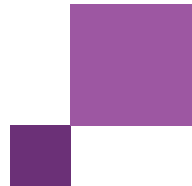


Figure 19	Modelled DPV bus with internal tripping signals	26
Figure 20	Block diagram of the DERAEMO model showing undervoltage and overvoltage multipliers (uv_mult, hv_mult).	26
Figure 21	Operational demand measurements (SCADA) – 13 February 2024	27
Figure 22	Map – 25 March 2024	31
Figure 23	PMU data vs playback simulation results: 11kV North Unley (N_UNLY)	32
Figure 24	Active power response of each model: 11kV North Unley (N_UNLY)	33
Figure 25	PMU data vs playback simulation results: 11kV Plympton (PLYMPTON)	33
Figure 26	Active power response of each model: 11kV Plympton (PLYMPTON)	34
Figure 27	Voltages – 25 March 2024	35
Figure 28	Active/reactive power – 25 March 2024 – 275kV City West PS to TIPS B Feeder	36
Figure 29	Active/reactive power – 25 March 2024 - 66 kV TIPS A to New Osborne PS Feeder	36
Figure 30	DPV measurements – South Australia total – 25 March 2024	37
Figure 31	Operational demand measurements (SCADA) – 25 March 2024	37
Figure 32	Map – 27 March 2024	41
Figure 33	PMU data vs playback simulation results: 11kV North Unley (N_UNLY)	42
Figure 34	Active power response of each model: 11kV North Unley (N_UNLY)	42
Figure 35	Voltages – 27 March 2024	44
Figure 36	Active/reactive power – 27 March 2024 – 275kV Northfield to TIPS A Feeder	44
Figure 37	Active/reactive power – 27 March 2024 – 66kV TIPS A to Port Adelaide North Substation Feeder	45
Figure 38	DPV measurements – South Australia total – 27 March 2024	45
Figure 39	Operational demand measurements (SCADA) – 27 March 2024	46
Figure 40	North Unley – 25 March 2024 – Playback simulation	48
Figure 41	Swings in operational demand captured by measurements in different locations	49
Figure 42	Simulated South Australian total regional operational demand (pu): 25 and 27 March	50
Figure 43	Impact of fault severity and DPV penetration on operational demand swings	51
Figure 44	CMLD & DPV model performance across three disturbances	54

# 1 Introduction

Three recent power system incidents (on 13 February 2024, 25 March 2024 and 27 March 2024) showed significant relevant behaviours from distributed PV (DPV) and aggregate load, and therefore provide an important opportunity to test and validate the behaviour of dynamic models that are used to represent load and DPV in dynamic power system studies. This report presents validation of AEMO's Composite Load (CMLD) and distributed PV (DPV) models in PSS®E against measurements from these three recent events.

These validation studies build on previous reports that summarise the development and testing of these models, published in 2022 and 2024. This report should be read in conjunction with these earlier reports, which remain valid, and provide an overview of the models and how the parameters for these models were developed:

- AEMO (November 2022) PSS®E models for load and distributed PV in the NEM<sup>3</sup>.
- AEMO (June 2024) PSS®E composite load and distributed PV model updates<sup>4</sup>.

## Structure of this report

This report is structured as follows:

- Section 2 summarises the validation studies against the incident in Victoria on 13 February 2024
- Section 3 summarises the validation studies against the incident in South Australia on 25 March 2024
- Section 4 summarises the validation studies against the incident in South Australia on 27 March 2024
- Section 5 summarises the main outcomes from investigations on operational demand swings
- Section 6 summarises the combined findings on validation of the models from all three events as well as recommendations based on this analysis.
- Appendix A1 shows the report glossary.
- Appendix A2 shows the data sources used to estimate the behaviour of DPV and load during these incidents.

## Data sources

Data has been collected from various sources:

- to estimate the quantity and types of DPV and load installed in the system associated with each transmission bus (this data informs the bottom-up development of parameters used in the models), and
- to understand the behaviour of DPV and load in these three power system disturbances (the models are validated against these measurements).

The data sources used in this analysis are summarised in Appendix A2.

## Models applied for comparison

The studies tested the performance of the models in three combinations:

<sup>3</sup> <https://aemo.com.au/-/media/files/initiatives/der/2022/psse-models-for-load-and-distributed-pv-in-the-nem.pdf?la=en>

<sup>4</sup> [https://aemo.com.au/-/media/files/initiatives/der/2024/report---psse-composite-load-and-distributed-pv-model-updates\\_.pdf?la=en](https://aemo.com.au/-/media/files/initiatives/der/2024/report---psse-composite-load-and-distributed-pv-model-updates_.pdf?la=en)

- **CMLD + DPV:** The latest composite load (CMLD) and DPV models developed by AEMO were applied.
- **ZIP only:** The historical load modelling approach used by AEMO was applied. This uses a static load model representing loads as a combination of constant impedance (Z), constant current (I), and constant power (P) components. DPV is represented as negative ZIP load.
- **ZIP + DPV:** A combination of the static ZIP load model with the AEMO DPV model was applied. This case is used to illustrate the separate effects of the new DPV model from the new composite load model. This model configuration is not recommended for power system studies, since the new DPV model is designed to be applied in conjunction with the new composite load model.

The ZIP modelling approach is simpler and may remain appropriate for some purposes.

## 2 Victoria: 13 February 2024

### 2.1 Event overview

At 1308 hrs on 13 February 2024, there was a significant power system event in Victoria involving the trip of the Moorabool (MLTS) – Sydenham (SYTS) 500 kV No. 1 and 2 lines due to the failure of six 500 kV towers (three on each of the two 500 kV circuits) during a severe weather event near Geelong. This event had a significant impact on the Victorian power system including:

- The loss of approximately 2,690 MW of generation,
- Shake-off<sup>5</sup> of 1,294 MW of underlying load across Victoria<sup>6</sup>, and
- Shake-off of 424 MW of DPV generation across Victoria.

This represents one of the most significant generalised load shake-off events observed in the NEM.

Further detail is available in AEMO incident reports<sup>7,8</sup>. The most relevant event information used for replicating this event in PSS®E is summarised in **Table 1**.

**Table 1 Event summary – 13 February 2024**

<b>Date and time</b>	13 February 2024, 13:08
<b>Region</b>	Victoria
<b>Description of the event</b>	<p>Four disturbances occurred on MLTS – SYTS 500 kV lines:</p> <p><b>Fault 1 (13:08:45.645):</b> Two phase to earth fault on the MLTS – SYTS No. 1 line.</p> <ul style="list-style-type: none"> <li>• MLTS circuit breakers opened after 48 ms</li> <li>• SYTS circuit breakers opened after 50 ms</li> </ul> <p><b>Fault 2 (13:08:46.550):</b> Single phase to earth fault on the MLTS – SYTS No. 2 line.</p> <ul style="list-style-type: none"> <li>• MLTS circuit breakers opened after 50 ms</li> <li>• SYTS circuit breakers opened after 42 ms</li> </ul> <p><b>Fault 3 (13:08:49):</b> The SYTS circuit breakers auto reclosed on the No. 1 line.</p> <ul style="list-style-type: none"> <li>• SYTS circuit breakers opened and locked after 67 ms</li> <li>• MLTS circuit breakers are synchronise checked, so did not reclose</li> </ul> <p><b>Fault 4 (13:08:50):</b> The SYTS circuit breakers auto reclosed on the No. 2 line.</p> <ul style="list-style-type: none"> <li>• SYTS circuit breakers opened and locked after 79 ms</li> <li>• MLTS circuit breakers are synchronise checked, so did not reclose</li> </ul>
<b>Minimum voltage recorded</b>	0.63 pu positive sequence recorded at LYPS during Fault 3

<sup>5</sup> Shake-off: the reduction in load or distributed PV generation due to devices tripping during a disturbance. Load shake-off = load tripped off and DPV shake-off = PV generation lost.

<sup>6</sup> This differs from Incident Report for this event, as the calculation methodology is different. The calculation for underlying load loss in this report is operational demand decrease at the time of the event + DPV disconnection according to SCADA data = underlying load loss

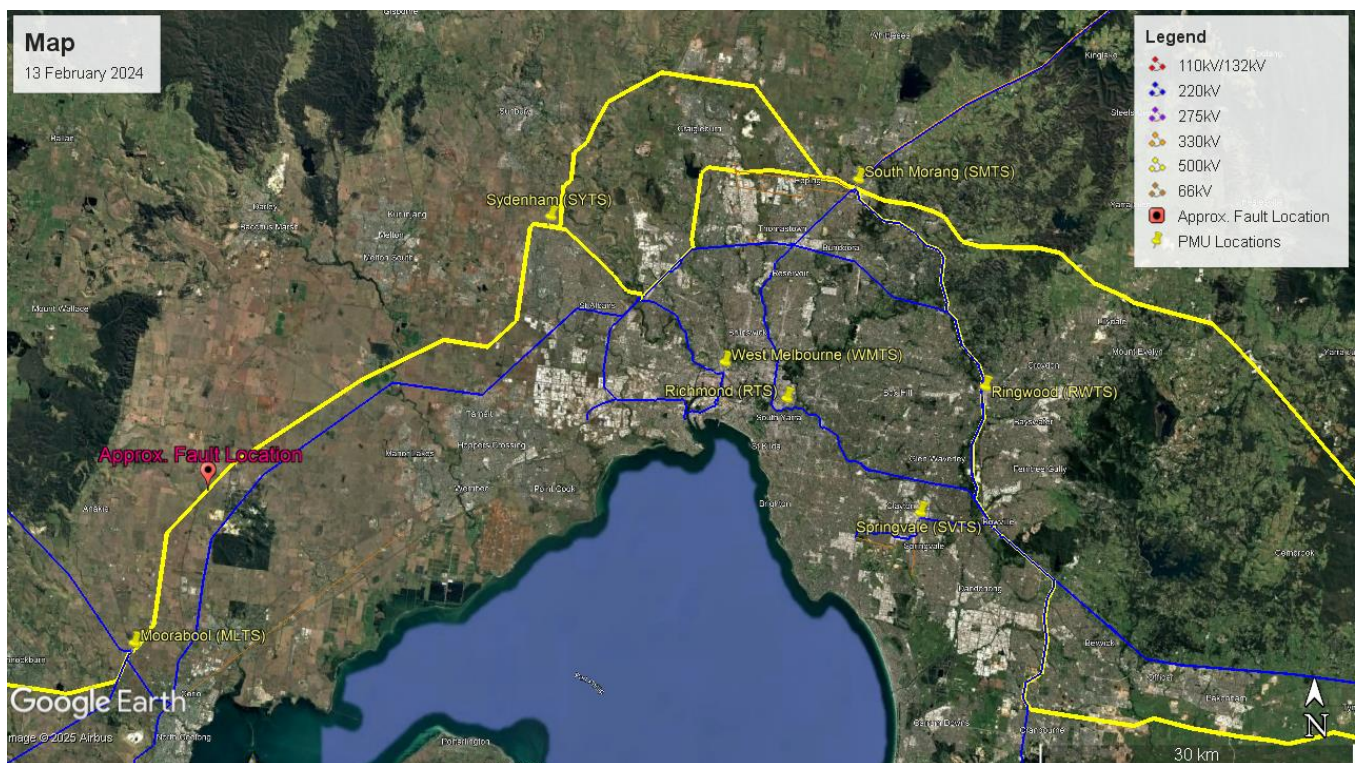
<sup>7</sup> AEMO (February 2024) Preliminary Report – Trip of Moorabool – Sydenham 500kV No 1 and No. 2 lines on 13 February 2024, [https://www.aemo.com.au/-/media/files/electricity/nem/market\\_notices\\_and\\_events/power\\_system\\_incident\\_reports/2024/preliminary-report--loss-of-moorabool---sydenham-500-kv-lines-on-13-feb-2024.pdf?la=en](https://www.aemo.com.au/-/media/files/electricity/nem/market_notices_and_events/power_system_incident_reports/2024/preliminary-report--loss-of-moorabool---sydenham-500-kv-lines-on-13-feb-2024.pdf?la=en)

<sup>8</sup> AEMO (November 2024) Non-credible islanding of the Jeeralang to Morwell 220kV network on 13 February 2024, [https://www.aemo.com.au/-/media/files/electricity/nem/market\\_notices\\_and\\_events/power\\_system\\_incident\\_reports/2024/non-credible-islanding-of-the-jeeralang-to-morwell-220-kv-network-on-13-february-2024.pdf?la=en](https://www.aemo.com.au/-/media/files/electricity/nem/market_notices_and_events/power_system_incident_reports/2024/non-credible-islanding-of-the-jeeralang-to-morwell-220-kv-network-on-13-february-2024.pdf?la=en)

<b>Installed capacity of DPV</b>		Total installed capacity in Victoria: 4929 MW <ul style="list-style-type: none"> <li>• 12% installed under AS/NZS4777.2:2020</li> <li>• 68% installed under AS/NZS4777.2:2015</li> <li>• 20% installed under AS/NZS4777.2:2005</li> </ul>
<b>Prior to the event</b>	<b>DPV generation</b>	2502 MW, 51% capacity factor <ul style="list-style-type: none"> <li>• Rooftop PV: 2,220 MW</li> <li>• PVNSG: 282 MW</li> </ul>
	<b>Operational demand</b>	7,704 MW
	<b>Underlying demand</b>	10,206 MW
<b>Estimated change (post disturbance vs pre disturbance)</b>	<b>DPV</b>	424 MW (range of 347-508 MW) decrease
	<b>Operational demand</b>	870 MW (range of 764-1,069 MW) decrease
	<b>Underlying demand</b>	1,294 MW (range of 1,111–1,577) decrease

The approximate location where the faults occurred is shown in Figure 5. The figure also shows the locations where relevant high-speed data was recorded, in proximity to the fault<sup>9</sup>.

Figure 5 Map – 13 February 2024



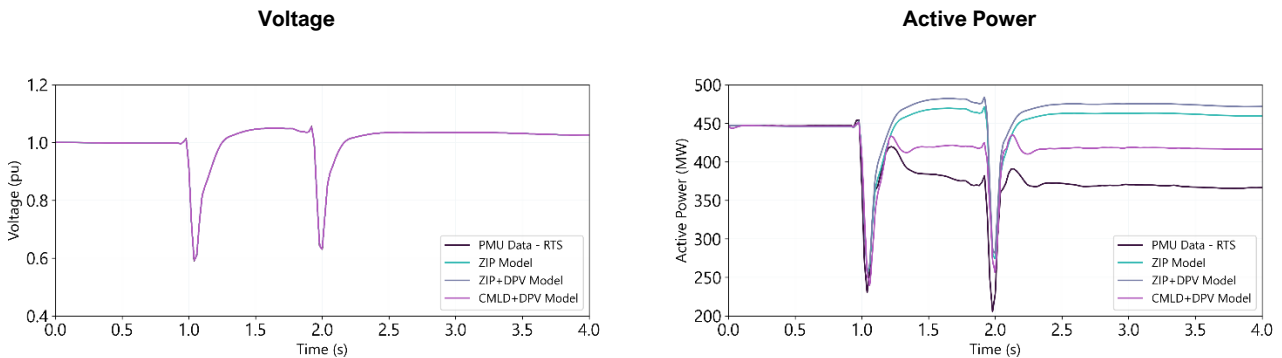
## 2.2 Representation of multiple faults

This event involved four faults in close succession. As an example, Figure 6 shows the voltage dips and the active power response measured at a radial aggregate load at the 220 kV Richmond Terminal Station (RTS). RTS serves

<sup>9</sup> HSM data was available at 500 kV Sydenham Terminal Station (SYTS), 500 kV Moorabool Terminal Station (MLTS), 500 kV South Morang Terminal Station (SMTS), 220 kV Richmond Terminal Station (RTS), 220 kV West Melbourne Terminal Station (WMTS), 220 kV Springvale Terminal Station (SVTS) and 220 kV Ringwood Terminal Station (RWTS).

Melbourne’s metro area with a mix of residential and commercial loads. At this location there is very minimal DPV capacity installed (it is estimated that DPV generation was contributing only 7% of the estimated underlying demand at this location pre-event). The load shake-off observed in response to each of the faults is evident in the lower active power settling level after each fault. The most significant load shake-off is observed in response to the third fault, which involved the most severe voltage dip.

**Figure 6 Voltage and active power at Richmond Terminal Station (RTS) 220 kV network**



The CMLD and DPV models have a known limitation for representing events with multiple faults in close succession. For events like this, these models will only calculate load and DPV shake-off associated with the first fault that falls below the relevant thresholds<sup>10</sup>, and then will not represent any further shake-off that may occur associated with any subsequent faults (further shake-off is “locked out” by the model logic). This means that the models will under-estimate the total amount of DPV and load shake-off if subsequent faults are deeper than the first fault. This is a known limitation of the model implementation in PSS®E.

For this reason, only the third voltage disturbance (which showed the deepest voltage depression in Melbourne CBD) was replicated in PSS®E to validate the models in system-wide studies. For playback cases (Single Load Infinite Bus), the third and fourth faults were replicated (which is also appropriate since the fourth fault was less severe). Modelling only the most severe fault (and possibly any subsequent less severe faults) provides the closest approximation to the real event for validation of the amount of shake-off, as well as validation of transient behaviours (which will be affected by the amount of shake-off that occurs).

### 2.3 Radial measurements (Single Load Infinite Bus simulations)

Table 2 summarises the locations where high speed (~20ms sampling rate) radial load measurements were available in this disturbance. These locations are particularly important for validation of load and DPV models, because the measurements provide a direct indication of the active and reactive power response of composite load and DPV in response to the disturbance experienced at that location, with less influence from the other complicating factors in the surrounding network.

<sup>10</sup> For example, the first undervoltage trip setting for motor A type loads is 0.75 pu with a trip delay of 0.06s. If the voltage disturbance seen by the CMLD model is below these thresholds, some portion of motor A type loads will trip and not recover. More information can be found in Table 1 on page 46 of the AEMO report “PSS®E composite load and distributed PV model updates”: [https://aemo.com.au/-/media/files/initiatives/der/2024/report---psse-composite-load-and-distributed-pv-model-updates\\_.pdf?la=en](https://aemo.com.au/-/media/files/initiatives/der/2024/report---psse-composite-load-and-distributed-pv-model-updates_.pdf?la=en)

RTS had low DPV penetration (7%), while RWTS had much higher DPV penetration (26%) at the time of the event. All of these locations recorded a minimum voltage of 0.6pu (positive sequence).

**Table 2 Terminal station summary of voltage sag, DPV participation and end-use load type**

Terminal Station	Details	End-Use Load Type	DPV generation pre-event (MW)	DPV contribution to underlying demand (%)	Minimum voltage recorded (pu)
RTS	220 kV Richmond Terminal Station	Mixed residential and commercial	33	7%	0.6
WMTS	220 kV West Melbourne Terminal Station	Mixed residential and commercial	32	12%	0.6
SVTS	220 kV Springvale Terminal Station	Predominantly residential	59	15%	0.6
RWTS	220 kV Ringwood Terminal Station	Predominantly residential	108	26%	0.6

For each of these locations, the voltage and frequency measurements recorded at the location during the third and fourth faults were played back with a Single Load Infinite Bus (SLIB) representation, to compare the active and reactive power response of the CMLD and DPV models in response to the voltage and frequency profiles recorded at this location.

### 2.3.1 Richmond Terminal Station (RTS)

Figure 7 illustrates the simulation results for RTS. The following observations can be made:

- **Active Power:** Active power dynamics are represented well by the CMLD+DPV models, and show a significant improvement compared with the ZIP model. Post-fault active power remains somewhat overestimated (the CMLD model is under-estimating load shake-off at this location).
- **Reactive Power:** Reactive power dynamics are represented very well by the CMLD+DPV models, and show a significant improvement compared with the ZIP model.
  - Following the clearance of the fourth fault, the models exhibit a transient peak in reactive power not reflected in the measured data. This discrepancy primarily arises from the dynamic reactive power response of motor loads, which the CMLD estimates constitute approximately 46% of the total end-use load in VIC. While this aggregate motor load response aligns accurately with observations for the initial fault, it overestimates reactive power peaks in subsequent faults. This behaviour is a recognised limitation of the CMLD model, which AEMO intends to address in future model revisions.
  - After the fourth fault clears, the models show a temporary peak in reactive power, which is not observed in the measured data following the fourth fault. This is primarily caused by the dynamic reactive power response of the motor loads, which is estimated in the CMLD to make up ~46% of the end-use load in VIC. While the collective motor response is appropriate for the first fault, it over-represents the peak reactive power in successive faults. This is a known limitation of the CMLD model which AEMO will aim to address in future revisions of the CMLD model.
  - The post-fault steady-state reactive power flows are very well captured by the CMLD+DPV models. By contrast, the ZIP and ZIP + DPV models under-represent both the magnitude and trajectory of reactive power changes during the fault and incorrectly predict a marginal increase, inconsistent with observations.

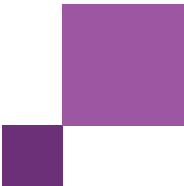


Figure 7 PMU data vs playback simulation results: Richmond Terminal Station (RTS)

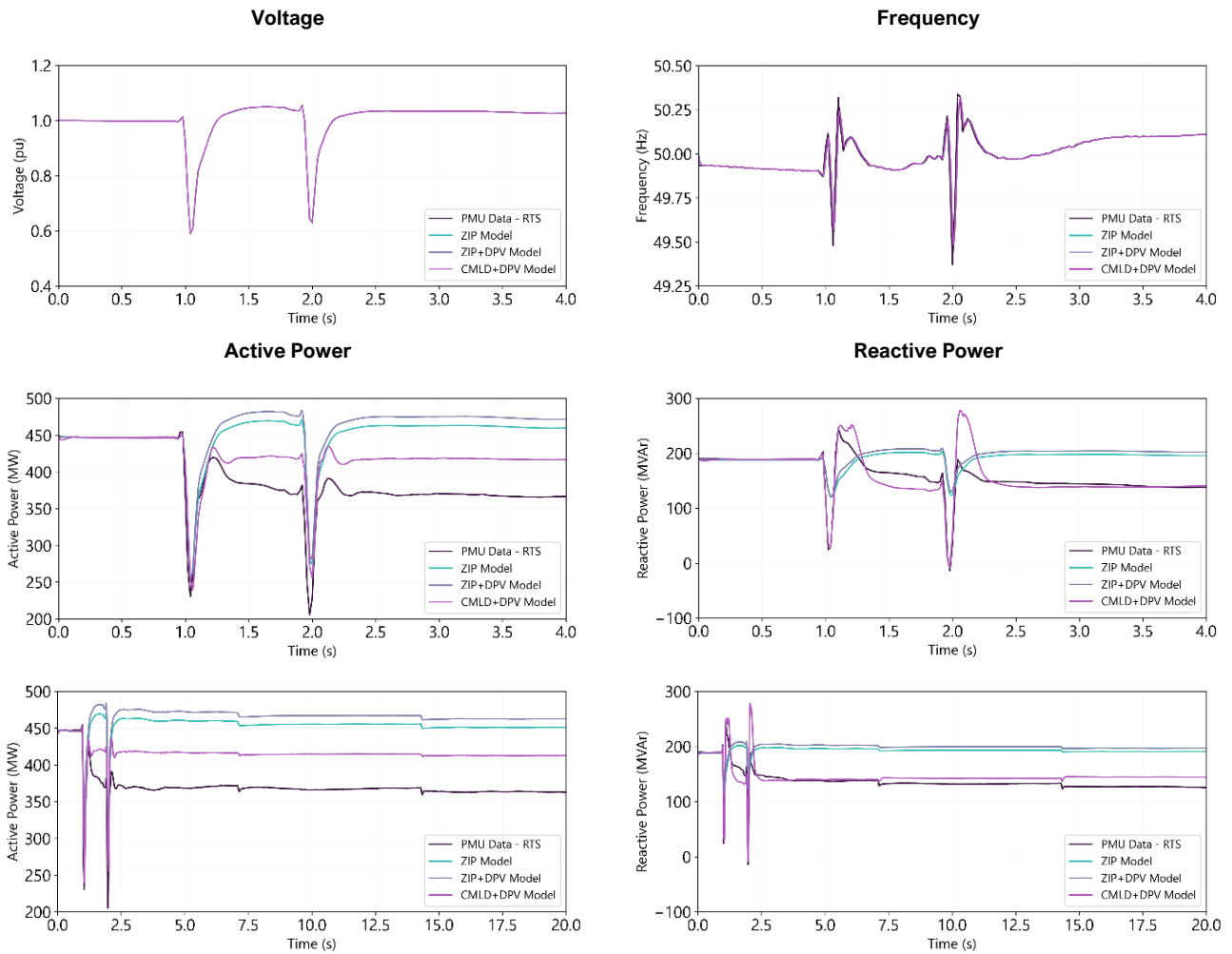


Figure 8 shows the simulation results for the individual CMLD and DPV models, illustrating the behaviour of each model separately in response to the third and fourth faults in a playback simulation at RTS. The figure shows the MW response of each model, as the change from an initial normalised value of 0 MW. The response at this location is dominated by the behaviour of the CMLD model, since the amount of DPV generating pre-fault is very small.

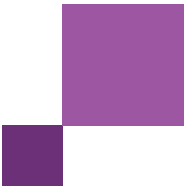
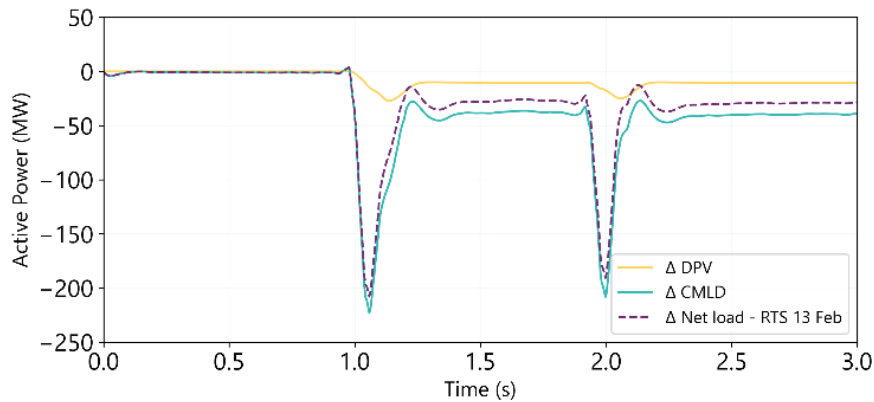


Figure 8 Active power response of each model: Richmond Terminal Station (RTS)

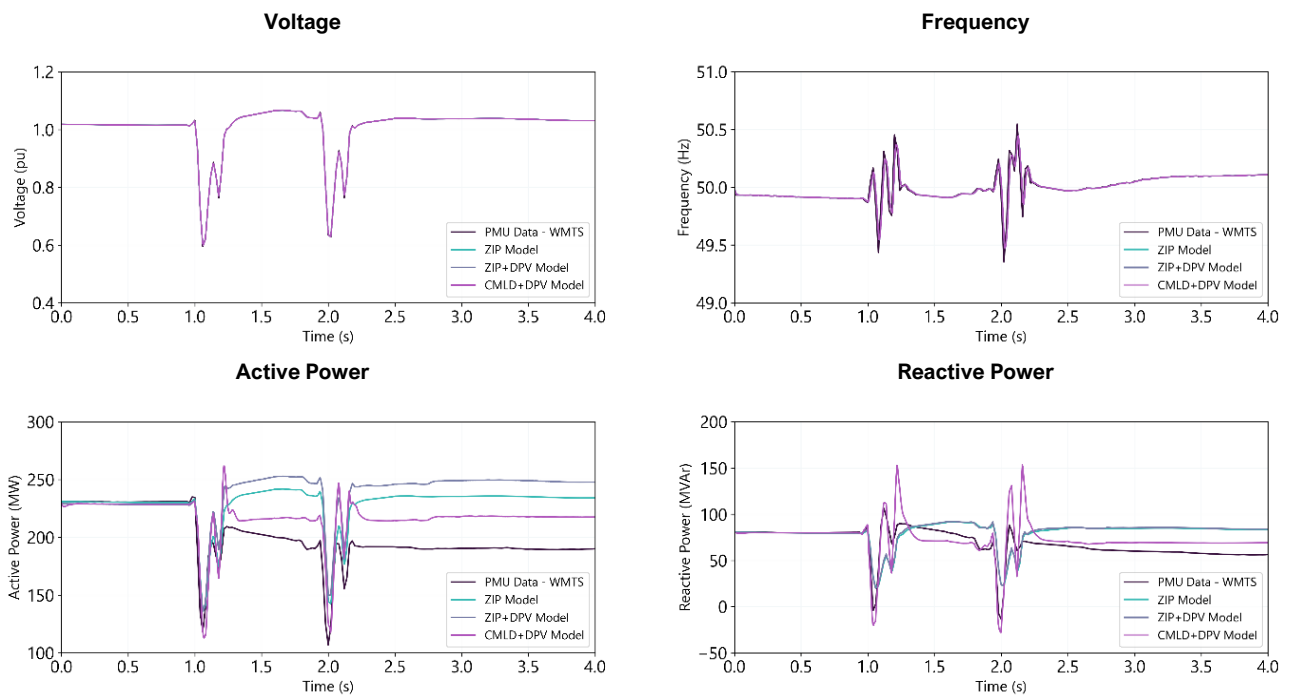


### 2.3.2 West Melbourne Terminal Station (WMTS)

Figure 9 presents the simulation results for West Melbourne Terminal Station (WMTS). Findings are similar to those for RTS:

- **Active Power:** The CMLD+DPV models show a significant improvement from the ZIP model, which does not capture any of the observed load shake-off. However, the CMLD model appears to underestimate load shake-off. High speed dynamics are also better captured by the CMLD+DPV models, compared with the ZIP model.
- **Reactive Power:** The CMLD+DPV models provide a significant improvement from the ZIP model, both in representing the high-speed dynamics during and post fault, as well as the steady-state settling values post fault. The CMLD model shows a transient spike after the fourth fault which is not visible in the measured data.

Figure 9 PMU data vs playback simulation results: West Melbourne Terminal Station (WMTS)



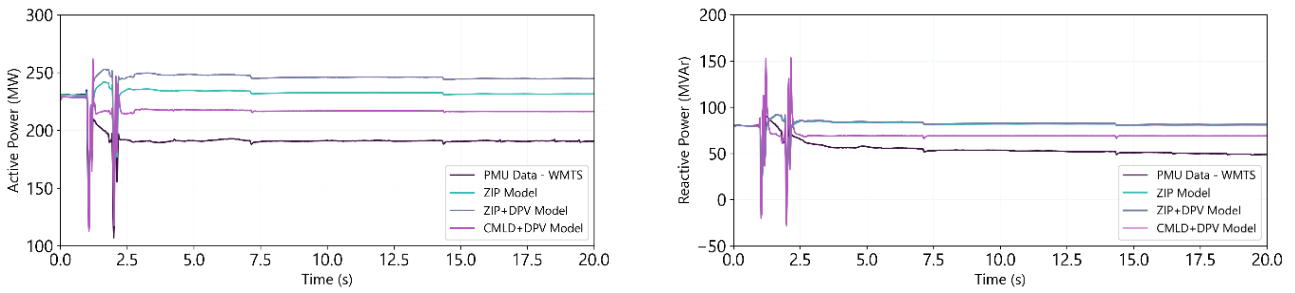
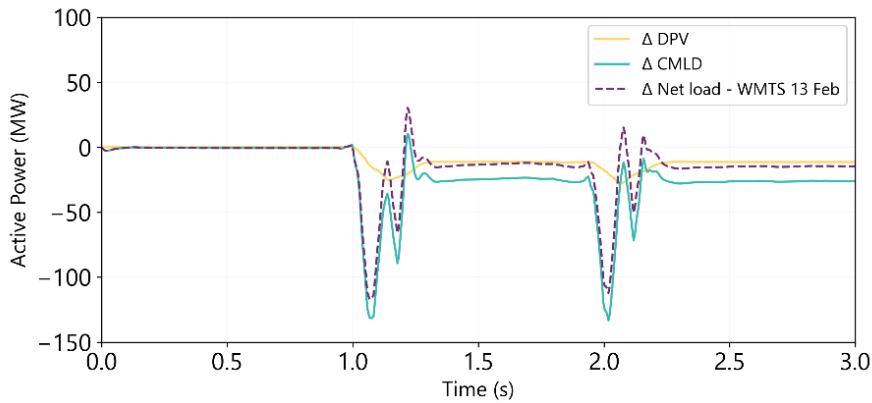


Figure 10 shows the separate responses of the CMLD and DPV models (normalised to 0 MW for the pre-fault values). The response at this location is dominated by the CMLD model, due to the very minimal amount of DPV installed at this location.

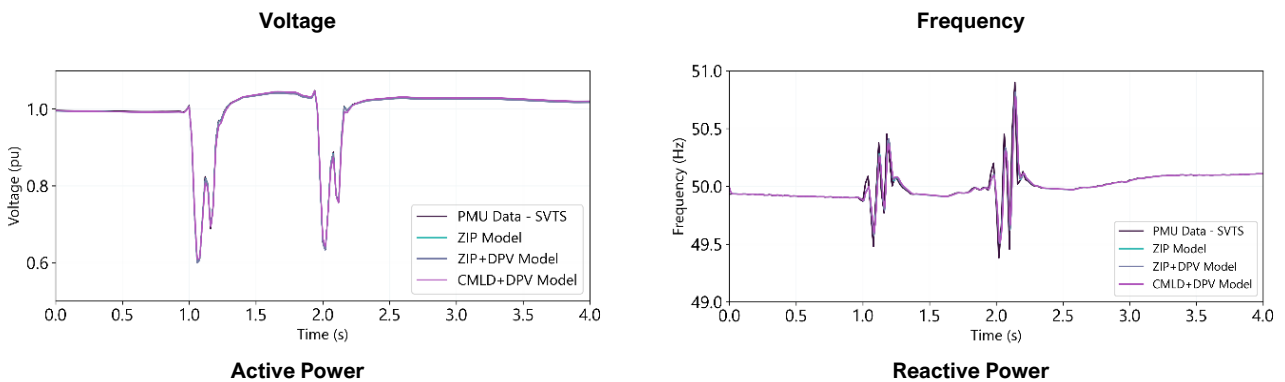
**Figure 10 Active power response of each model: West Melbourne Terminal Station (WMTS)**



### 2.3.3 Springvale Terminal Station (SVTS)

Figure 11 presents the simulation results for Springvale Terminal Station (SVTS). Findings are similar to those for RTS and WMTS, reinforcing the validation against multiple locations with different kinds of loads, and differing levels of DPV generation. Like RWTS, SVTS primarily serves Melbourne’s metro area, characterised by a mix of residential loads. This location had a somewhat higher level of DPV penetration.

**Figure 11 PMU data vs playback simulation results: Springvale Terminal Station (SVTS)**



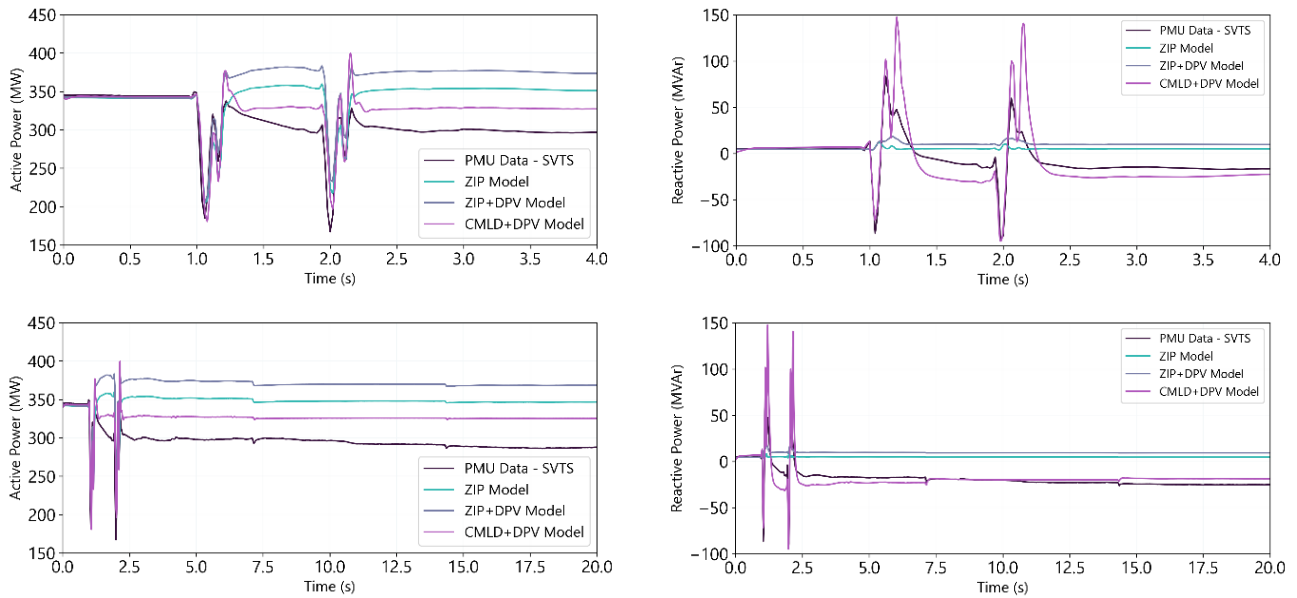
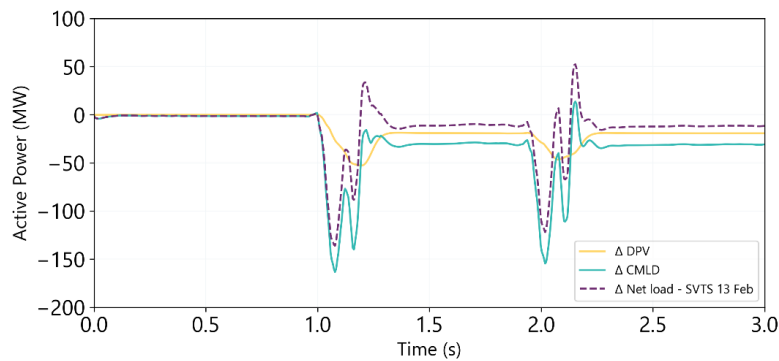


Figure 12 shows the normalised active power response of each of the CMLD and DPV models, showing the somewhat more significant contribution of DPV at this location (although the response remains dominated by the CMLD model).

**Figure 12 Active power response of each model: Springvale Terminal Station (SVTS)**



### 2.3.4 Ringwood Terminal Station (RWTS)

Figure 13 presents the simulation results for RWTS. RWTS serves Melbourne’s metro area, characterised by a mix of residential loads. At this location, DPV is estimated to be delivering 26% of underlying demand pre-fault, and therefore makes a more significant contribution to the dynamics at this location. Observations are as follows:

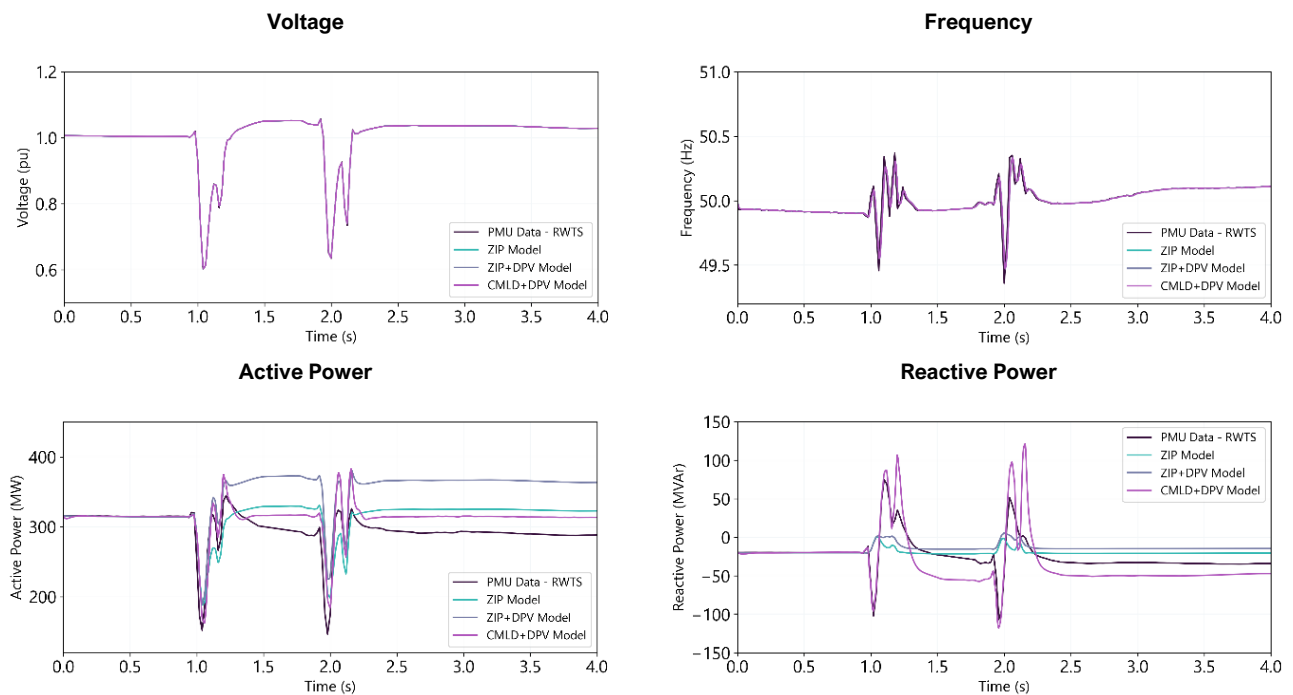
- **Active Power**
  - Transient behaviours are better represented by CMLD+DPV models, compared with the ZIP models.
  - At this location, the measurements indicate a small reduction in net load (comparing pre vs post fault active power levels), suggesting that load shake-off exceeded DPV shake-off. The CMLD and DPV models predict similar levels of shake-off at this location, leading to minimal change in net load. This delivers a

similar outcome to the ZIP model, which does not predict any shake-off (and therefore coincidentally delivers a reasonably accurate steady-state post fault outcome overall for this particular location). The least accurate representation is the ZIP+DPV model, which shows the DPV shake-off but does not represent any load shake-off, and therefore predicts a significant increase in active power post fault which is not observed in measurements. This illustrates the importance of application of the CMLD model when using the DPV model, if there are power system circumstances that will lead to DPV shake-off.

• **Reactive Power**

- Transient behaviours are significantly better represented by the CMLD+DPV models, compared with the ZIP models.
- In the steady state (shown in the bottom right panel), the CMLD+DPV models accurately represent the reduction in reactive power flows across the feeder, but this occurs more quickly in the model (5s) compared to the PMU data (8s). The ZIP and ZIP+DPV models maintain reactive power flows at pre-fault levels, failing to represent the observed reduction and diverging significantly from measurements.
- The net steady-state active power outcome of the CMLD+DPV model was similar to ZIP due to offsetting errors (CMLD+DPV models predicted both load and PV drop, which cancelled each other out). In isolated cases a simple ZIP model can appear to perform “well” only because it misses both effects.

**Figure 13** PMU data vs playback simulation results: Ringwood Terminal Station (RWTS)



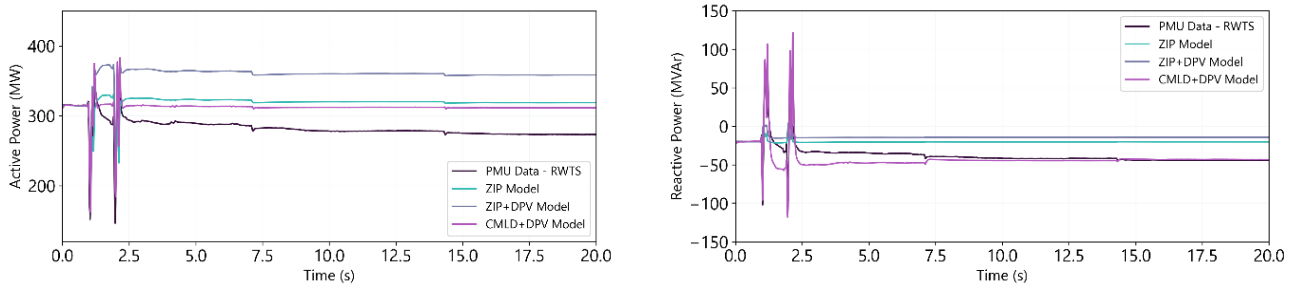
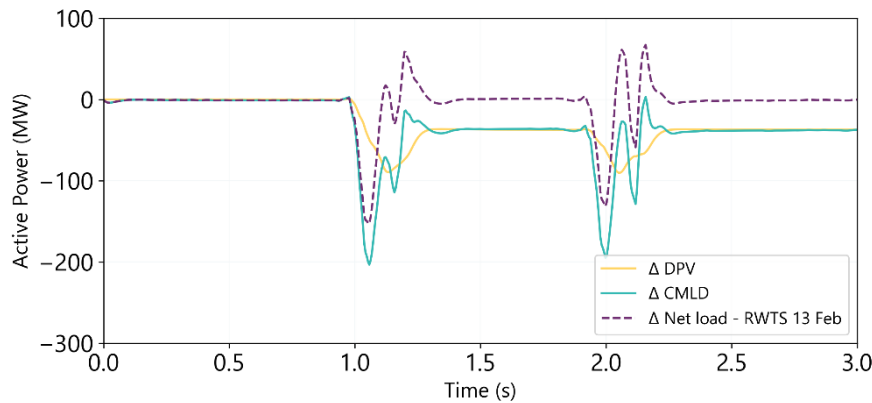


Figure 14 shows the separate normalised responses of the DPV and CMLD models. At this location both are influential.

**Figure 14 Active power response of each model: Ringwood Terminal Station (RWTS)**



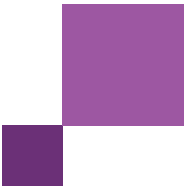
## 2.4 System-wide studies

### 2.4.1 Replication in PSS®E

The following simulation sequence was performed in PSS®E to replicate this case for system-wide studies.

**Table 3 Simulation event summary – 13 February 2024**

Time (s)	Events/comments
<b>Before Simulation</b>	The third fault occurred roughly one-third of the way along the 500 kV MLTS–SYTS line from the MLTS end (Figure 5). To replicate its location in PSS®E, a bus was inserted at 33% of the line length to serve as the fault location, and the line impedance was split in a 1:2 ratio.
<b>0</b>	Start simulation.
<b>1.000</b>	Apply a 3-phase (3P) fault on the 500 kV MLTS–SYTS No. 1 branch at the identified fault location. Although the actual fault measurement indicated a two-phase-to-ground (2PG) fault, a bolted fault did not provide a sufficiently severe voltage depression. Therefore, a 3P fault was used to better match the observed positive sequence voltage depressions. The fault impedance was then adjusted to align the simulated voltage response at the 500 kV South Morang Terminal Station (SMTS) bus with PMU data for Fault 3.
<b>1.067</b>	Clear the 3P fault on the 500 kV MLTS–SYTS No. 1 branch on the SYTS end and disconnect the branch between the fault bus and bus 376090.
<b>10</b>	End simulation



## 2.4.2 High speed measurements

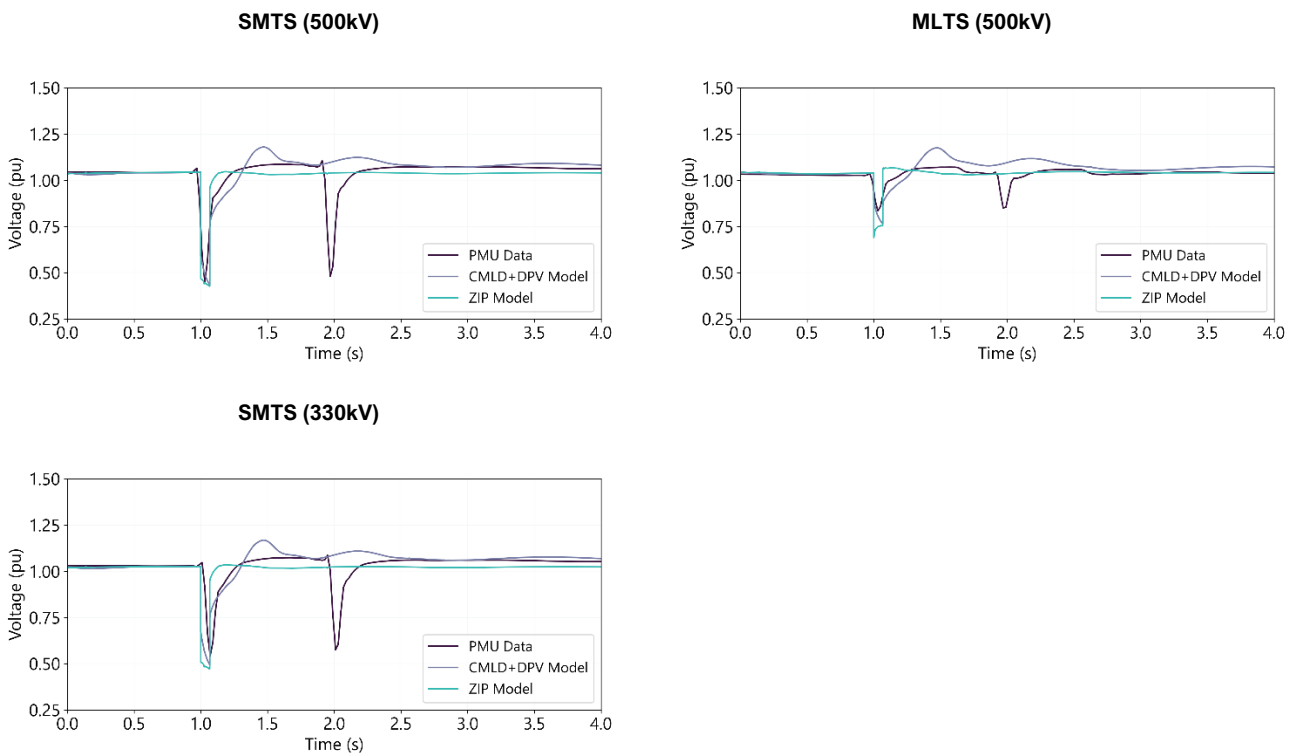
### Voltages

Figure 15 shows the voltage PMU data at various transmission terminal stations for Faults 3 and 4. Due to model limitations<sup>11</sup>, only the largest (third) fault was simulated to capture the majority of the shake-off<sup>12</sup> (see section 2.2 for reason). SMTS is located on the 500 kV network near the Melbourne metropolitan area, a major load and DPV centre.

During this disturbance:

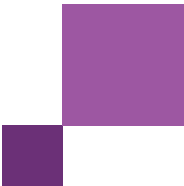
- The ZIP model predicts a faster voltage recovery than what the PMU data indicates. The CMLD + DPV models better capture the short delay in voltage recovery.
- The CMLD + DPV models show a temporary post-fault voltage overshoot not seen in the PMU data. This overshoot briefly exceeds the normal voltage range of 0.9 to 1.1 pu.
- Both the CMLD + DPV and ZIP models accurately represent the steady-state voltage at 60 seconds (not shown).

**Figure 15** Voltages – 13 February 2024



<sup>11</sup> The DPV and CMLD models in PSS®E can only represent the shake-off behaviour of a single fault and are unable to capture the additional shake-off likely caused by multiple faults. See section 2.2 for more information.

<sup>12</sup> See section 2.2, which covers the known limitations of the CMLD and DPV models for representing events with multiple faults in close succession.



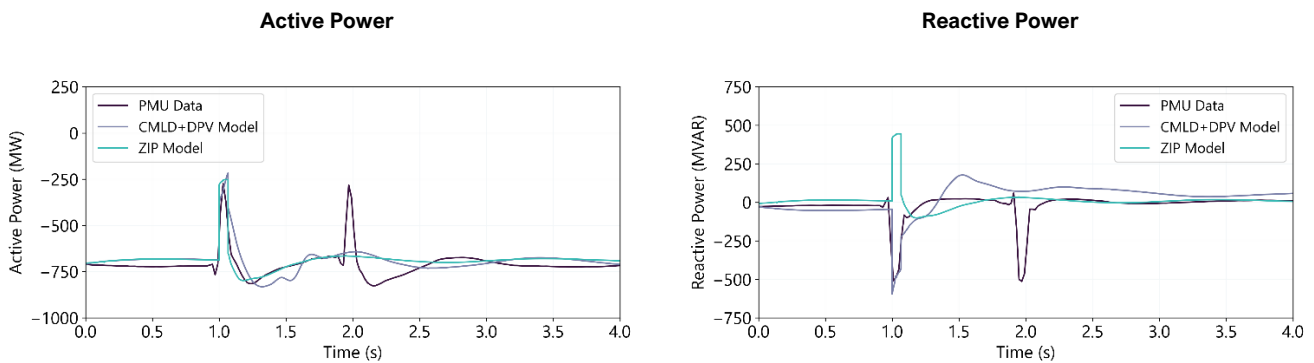
### Active and reactive power flows

Figure 16 shows the active and reactive power measurements on the 500 kV SMTS–HWTS line near the faulted area. Key observations include:

- **Active Power:** Both the ZIP and CMLD+DPV models closely match the PMU measurements during and after the fault.
- **Reactive Power:**
  - The ZIP model significantly misrepresents the reactive power trajectory during the fault. In contrast, the CMLD+DPV model much more accurately reflects the PMU data.
  - The CMLD+DPV model exhibits a small post-fault overshoot that is not seen in the PMU data (but still provides a significant improvement in representation of transient behaviours during and post fault, compared with the ZIP model).

Similar trends were observed at 500 kV SYTS.

**Figure 16** Active/reactive power – 13 February 2024 – 500kV SMTS to HWTS Feeder

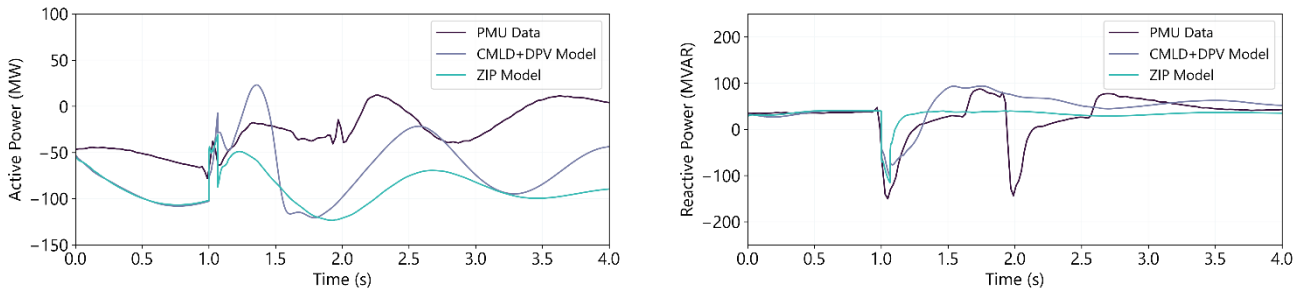
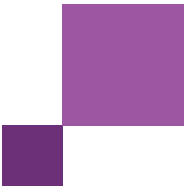


Post fault steady-state active and reactive power measured at 60s (not shown) were well represented by both models at 500 kV SMTS and 500 kV SYTS.

Figure 17 shows the active and reactive power measurements on the 500 kV MLTS–HGTS line near the faulted area. Both the ZIP and CMLD+DPV models represent the general trajectory of active and reactive power during and immediately following the fault, while the CMLD+DPV model better represents the transient amplitude.

**Figure 17** Active/reactive power – 13 February 2024 – 500kV MLTS to HGTS Feeder

**Active Power** **Reactive Power**



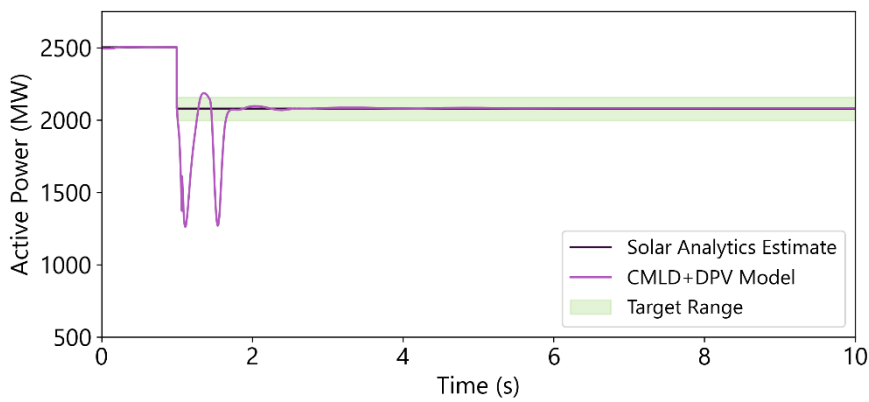
Post fault steady-state active and reactive power measured at 60s (not shown) were better represented by the CMLD+DPV model at 500 kV MLTS.

### 2.4.3 DPV shake-off

In this event, it is estimated that DPV generation across Victoria reduced by approximately 424 MW (based on observed shake-off of a sample of systems, upscaled to represent the Victorian fleet, and including PVNSG).

Figure 18 compares this estimated change in total DPV generation in Victoria with modelled results. The DPV model accurately estimates the DPV shake-off within the identified target range.

**Figure 18** DPV measurements – Victoria total – 13 February 2024



A single fault was used to generate the results shown in Figure 18. The second drop in active power is due to an overvoltage condition following the voltage overshoot. Figure 19 illustrates this effect, showing the active power, bus voltage, and internal under and overvoltage multipliers for a representative DPV bus.

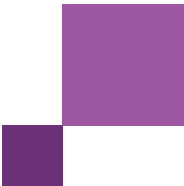
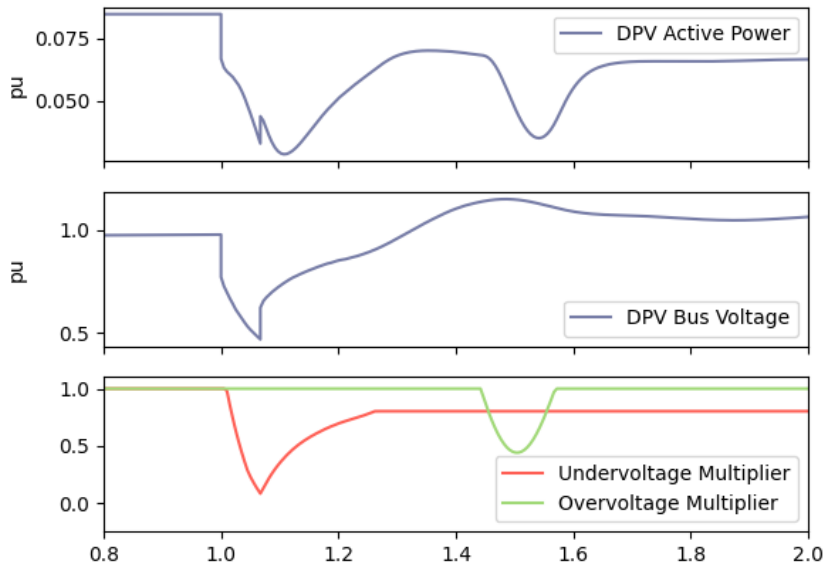


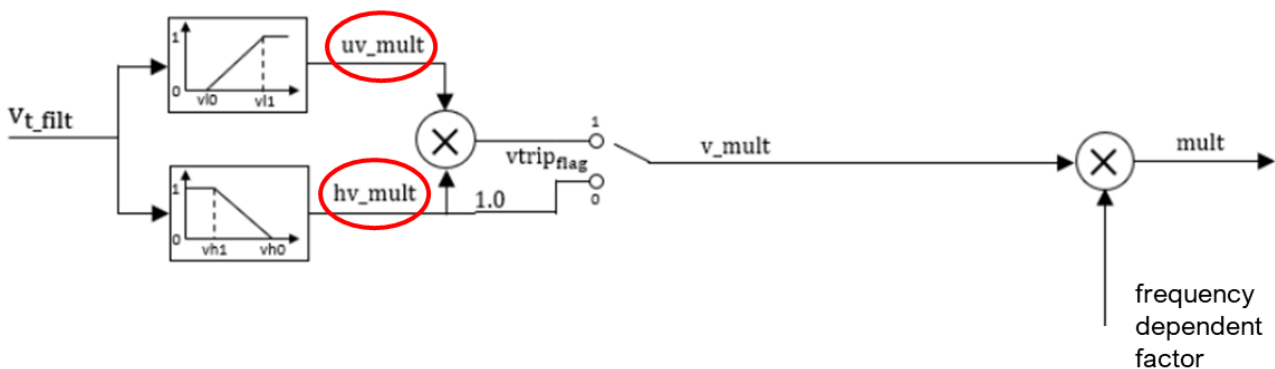
Figure 19 Modelled DPV bus with internal tripping signals



As shown in the block diagram in Figure 20, these internal undervoltage and overvoltage signals directly influence the modelled DPV active power. Notably, the under (UV) and overvoltage (HV) multipliers can reduce power output partially (rather than triggering a full trip) when the bus voltage temporarily deviates from nominal. In this case, the over-voltage multiplier temporarily reduces the DPV model active power (producing a second transient dip). However, the steady-state reduction in DPV active power is an outcome of the under-voltage condition only, as shown by the red (undervoltage, with steady-state reduction) and green (overvoltage, with no reduction) multipliers in Figure 20.

The available DPV datasets that measure DPV responses in the field do not differentiate between tripping caused by overvoltage versus undervoltage or between partial power reductions and full disconnections. These datasets also do not have sufficient resolution to observe DPV transient behaviours. This means it is not possible (based on present datasets) to determine if the field measurements had a temporary contribution of tripping related to over-voltage as well as under-voltage.

Figure 20 Block diagram of the DERAEMO model<sup>13</sup> showing undervoltage and overvoltage multipliers (uv\_mult, hv\_mult).



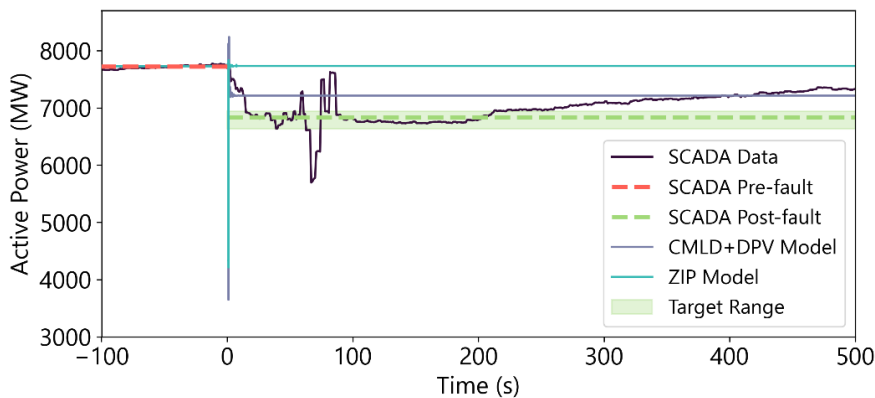
<sup>13</sup> <https://aemo.com.au/-/media/files/initiatives/der/2022/psse-models-for-load-and-distributed-pv-in-the-nem.pdf?la=en>

### 2.4.4 Load shake-off

Figure 21 compares SCADA-measured operational demand in Victoria against the net total active power response predicted by the CMLD+DPV model. Following the disturbance, operational demand dropped by approximately 870 MW, then gradually recovered to its pre-fault level over the next 10 minutes (not shown).

Because of inherent inaccuracies in SCADA data, the precise magnitude of net disconnection is uncertain; therefore, a target range is shown, based on the minimum and maximum SCADA readings in the first 50 seconds after the fault.

**Figure 21** Operational demand measurements (SCADA) – 13 February 2024



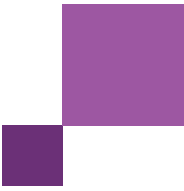
In this event:

- The ZIP model does not show any shake-off, and completely fails to represent the observed 870 MW reduction in operational demand. This represents a significant misrepresentation of power system behaviour in this event and illustrates the importance of applying the CMLD+DPV models for representing events of this type (where shake-off is significant).
- The CMLD model predicts a total load loss of 909 MW, offset by 419 MW of DPV disconnection, resulting in a net 490 MW decrease — less than the 870 MW drop indicated by SCADA measurements. This represents a considerable improvement compared with the ZIP model but highlights the considerable error margins that remain when attempting to model complex composite load behaviours.

Table 4 provides a comparison of these estimates.

**Table 4** Summary of change in demand and distributed PV – 13 February 2024

	Actuals (estimated)	CMLD + DPV prediction
<b>Change in DPV generation</b>	424 MW (347 – 508 MW) decrease (estimated from Solar Analytics sample)	419 MW decrease (underestimates by 5 MW)
<b>Change in underlying demand</b>	1,294 MW (1,111 – 1,577 MW) decrease (estimated from SCADA & Solar Analytics)	909 MW decrease (underestimates by 385 MW)
<b>Change in operational demand</b>	870 MW (764 – 1,069 MW) decrease (estimated from SCADA)	490 MW decrease (underestimates by 380 MW)



### 2.4.5 Summary of model performance in system-wide cases

Table 5 summarises the performance of the models for this event. Colour coded ratings indicate how well the CMLD model aligns with PMU measurements. Green denotes a good match, orange signifies a fair match, and red indicates a poor match.

A cross (X) identifies instances where the ZIP model outperforms the CMLD model, a single tick (✓) signifies that the CMLD model performs at least as well as the ZIP model, and a double tick (✓✓) highlights cases where the CMLD model significantly outperforms the ZIP model.

For this event, the CMLD+DPV models perform at least as well as the ZIP model across almost all characteristics (except voltage overshoot), and significantly outperform the ZIP model in many characteristics. The CMLD+DPV models also provide a good match across many characteristics. This indicates that the CMLD+DPV model representation offers a considerable improvement compared with the prior ZIP model.

**Table 5 Assessment of model performance – 13 February 2024**

Quantity	Characteristic	CMLD + DPV estimates	CMLD + DPV model equal (✓) or better (✓✓) than ZIP?	Commentary
<b>Voltages</b>	Voltage overshoot	Fair match	X	The CMLD + DPV marginally overestimates peak voltage overshoot magnitude.
	Voltage recovery rate	Fair match	✓✓	CMLD + DPV comparable to PMU.
	Steady-state post disturbance	Good match	✓	CMLD + DPV voltages are accurate (settles to within 5% of the PMU data for all voltage channels).
<b>Active power</b>	During dynamic state	Good match	✓	CMLD + DPV has a similar trajectory and magnitude to the PMU data.
	Steady-state post disturbance	Good match	✓✓	CMLD + DPV aligned with PMU.
<b>Reactive power</b>	During dynamic state	Good match	✓✓	CMLD + DPV has a similar trajectory and magnitude to the PMU data, while the ZIP is unable to represent the trajectory.
	Steady-state post disturbance	Good match	✓	CMLD + DPV aligned with PMU.
<b>DPV</b>	DPV change	Good match	✓✓	Estimated actuals: 424 MW decrease DPV model: 419 MW decrease The DPV model overestimates DPV disconnection by 5 MW and within range.
<b>CMLD</b>	Underlying load change	Fair match	✓✓	Estimated actuals: 1294 MW decrease CMLD: 909 MW decrease The CMLD underestimates load disconnection by 385 MW but provides a considerable improvement on the ZIP model which shows no load disconnection.
<b>Operational Demand</b>	Net load change	Fair match	✓✓	Estimated actuals: 870 MW decrease CMLD + DPV model: 490 MW decrease The CMLD + DPV model underestimates net load change by 380 MW but provides a considerable improvement on the ZIP model which shows no change to operational demand.

## 3 South Australia: 25 March 2024

### 3.1 Event overview

On 25 March 2024, Torrens Island Power Station B (TIPS B) experienced a trip involving the 275 kV circuit breakers CB BW3 and CB BC3. The 275 kV network at Parafield Gardens (PARA) subsequently recorded a minimum positive-sequence voltage of 0.6 pu. In response, the South Australian region saw a net load gain of +118 MW, attributed to DPV generation loss exceeding load shake-off.

In this event, DPV inverters under 30 kW installed after April 2023 showed minimal shake-off, while a 40% shake-off occurred among 30–100 kW inverters regardless of installation date.

Further details are provided in the incident report<sup>14</sup> and its addendum<sup>15</sup>.

**Table 6 Event summary – 25 March 2024**

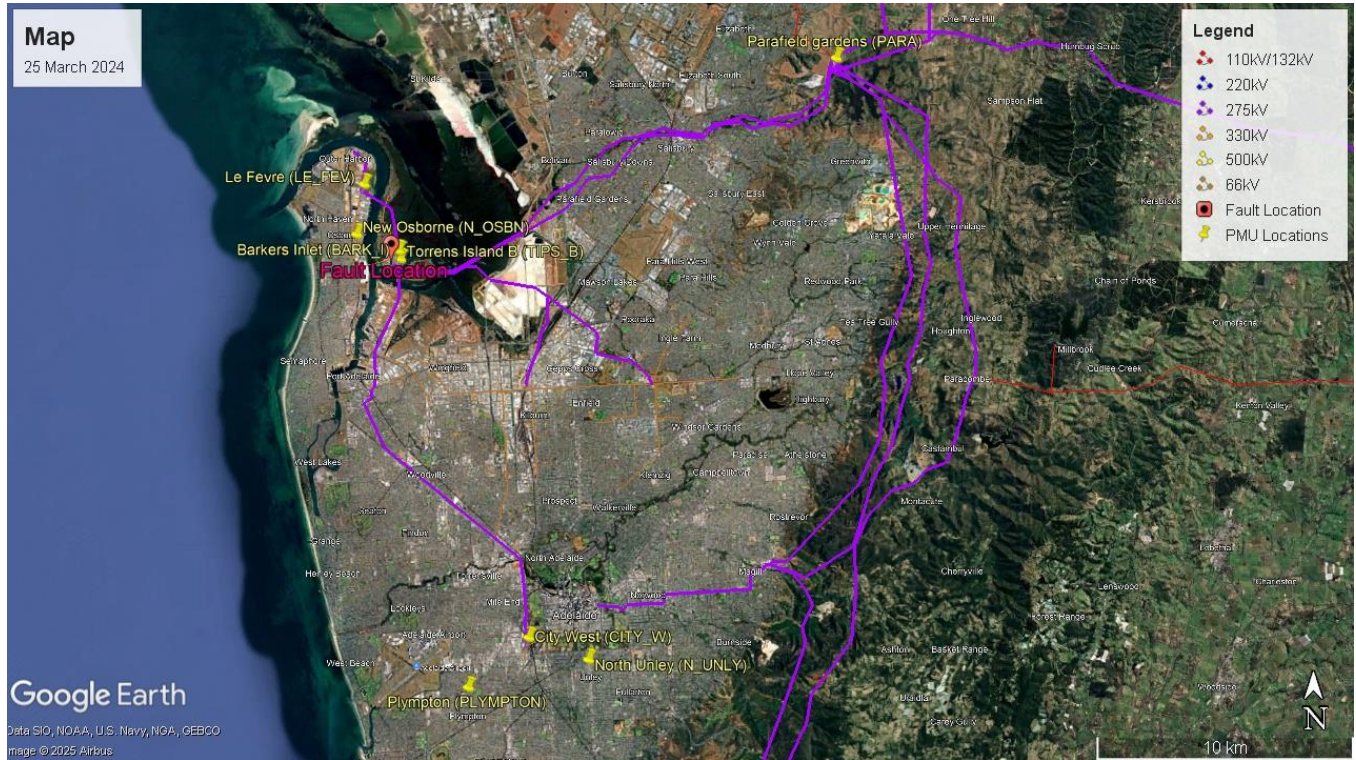
<b>Date and time</b>		25 March 2024, 14:12
<b>Region</b>		South Australia
<b>Description of the event</b>		<p>An internal fault in the 'V' phase Current Transformer (CT) occurred on the west side of the TIPS B 275kV CB BC3 at 14:12. The fault resulted in the loss of one generating unit in South Australia.</p> <p>The event is summarised as:</p> <ul style="list-style-type: none"> <li>• Trip of TIPS B unit 3.</li> <li>• Trip of TIPS B 275 kV CB BC3 &amp; BW3.</li> <li>• A single phase on the LeFevre – TIPS B 275 kV line (TIPS B 275kV CB BE3 &amp; LeFevre 275kV CB 6570) tripped and auto-reclosed successfully from both ends.</li> </ul>
<b>Minimum voltage recorded</b>		0.6 pu positive sequence recorded at Para 275 kV
<b>Installed capacity of DPV</b>		<p>Total installed capacity in South Australia: 2780 MW</p> <ul style="list-style-type: none"> <li>• 25% installed under AS4777.3:2005</li> <li>• 64% installed under AS4777.2:2015</li> <li>• 11% installed under AS4777.2:2020</li> </ul>
<b>Prior to the event</b>	<b>DPV</b>	<p>1478 MW, 53% capacity factor</p> <ul style="list-style-type: none"> <li>• Rooftop PV: 1286 MW</li> <li>• PVNSG: 192 MW</li> </ul>
	<b>Operational demand</b>	392 MW
	<b>Underlying demand</b>	1870 MW
<b>Estimated change (post disturbance vs pre disturbance)</b>	<b>DPV</b>	222 MW (range of 192-266 MW) decrease
	<b>Operational demand</b>	118 MW (range of 108-133 MW) increase
	<b>Underlying demand</b>	104 MW (range of 59-158 MW) decrease

<sup>14</sup> AEMO (September 2024) 275kV current transformer failures in South Australia 14-27 March, [https://aemo.com.au/-/media/files/electricity/nem/market\\_notices\\_and\\_events/power\\_system\\_incident\\_reports/2024/report-on-current-transformer-failures-during-march-2024-in-south-australia.pdf?la=en&hash=E0EE498E5BBDBF24F0CCA7CEE4E7EE08](https://aemo.com.au/-/media/files/electricity/nem/market_notices_and_events/power_system_incident_reports/2024/report-on-current-transformer-failures-during-march-2024-in-south-australia.pdf?la=en&hash=E0EE498E5BBDBF24F0CCA7CEE4E7EE08)

<sup>15</sup> AEMO (October 2024) Addendum on DPV and load behaviour: 275kV current transformer failures in South Australia 14-27 March 2024, [https://aemo.com.au/-/media/files/electricity/nem/market\\_notices\\_and\\_events/power\\_system\\_incident\\_reports/2024/addendum-on-dpv-and-load-behaviour275-kv-current-transformer-failures-in-south-australia-1427-march.pdf](https://aemo.com.au/-/media/files/electricity/nem/market_notices_and_events/power_system_incident_reports/2024/addendum-on-dpv-and-load-behaviour275-kv-current-transformer-failures-in-south-australia-1427-march.pdf)

Figure 22 shows a map, indicating the location of the disturbance (Torrens Island Power Station B), and the locations where high-speed data measurements were available<sup>16</sup>.

Figure 22 Map – 25 March 2024



### 3.2 Radial measurements (Single Load Infinite Bus simulations)

For this event, radial high-speed measurements were available at two locations: North Unley and Plympton (both in the 11kV distribution network). These are summarised in Table 7. Both locations have high levels of DPV generation, which was providing a high contribution to underlying demand at the time of this event.

Table 7 Terminal station summary of voltage sag, DPV participation and end-use load type

Terminal Station	End-Use Load Type	Pre-Fault Active Power (MW)	DPV Generation (MW)	DPV contribution to underlying demand (%)	Minimum voltage recorded (pu)
11 kV North Unley	Predominantly residential	0.78	5.3	87%	0.55
11 kV Plympton	Mixed residential and commercial	-0.47	7.7	106%	0.64

#### 3.2.1 11 kV North Unley (N\_UNLY)

Figure 23 presents the playback simulation results for the 11 kV North Unley feeder in South Australia. This feeder primarily serves suburban residential loads, with high levels of DPV penetration at the time of the event.

<sup>16</sup> HSM data is available at 275 kV Lefevre, 275 kV Barkers Inlet, 275 kV Parafield Gardens, 275 kV New Osborne, 275 kV Torrens Island B, 275 kV City West, 11 kV Plympton, and 11 kV North Unley

Observations are as follows:

- Active Power:** At this location, the DPV shake-off exceeds the load shake-off, resulting in an increase in active power post fault. The ZIP model fails to capture this steady-state change in active power. The CMLD+DPV model provides a considerable improvement. The steady-state active power level post fault is slightly overestimated and reaches the steady-state level a little too quickly (while measurement data takes longer to settle). The ZIP model also fails to reproduce the significant rise or “swing” in active power post fault, but this is well represented by the CMLD+DPV models; this is discussed further below.
- Reactive Power:** The ZIP model entirely fails to capture the transient behaviours during and post fault; these are much better captured by the CMLD+DPV model. Both models provide a reasonable representation of the post fault steady-state reactive power condition, which is relatively unchanged from pre-fault conditions.

Figure 23 PMU data vs playback simulation results: 11kV North Unley (N\_UNLY)

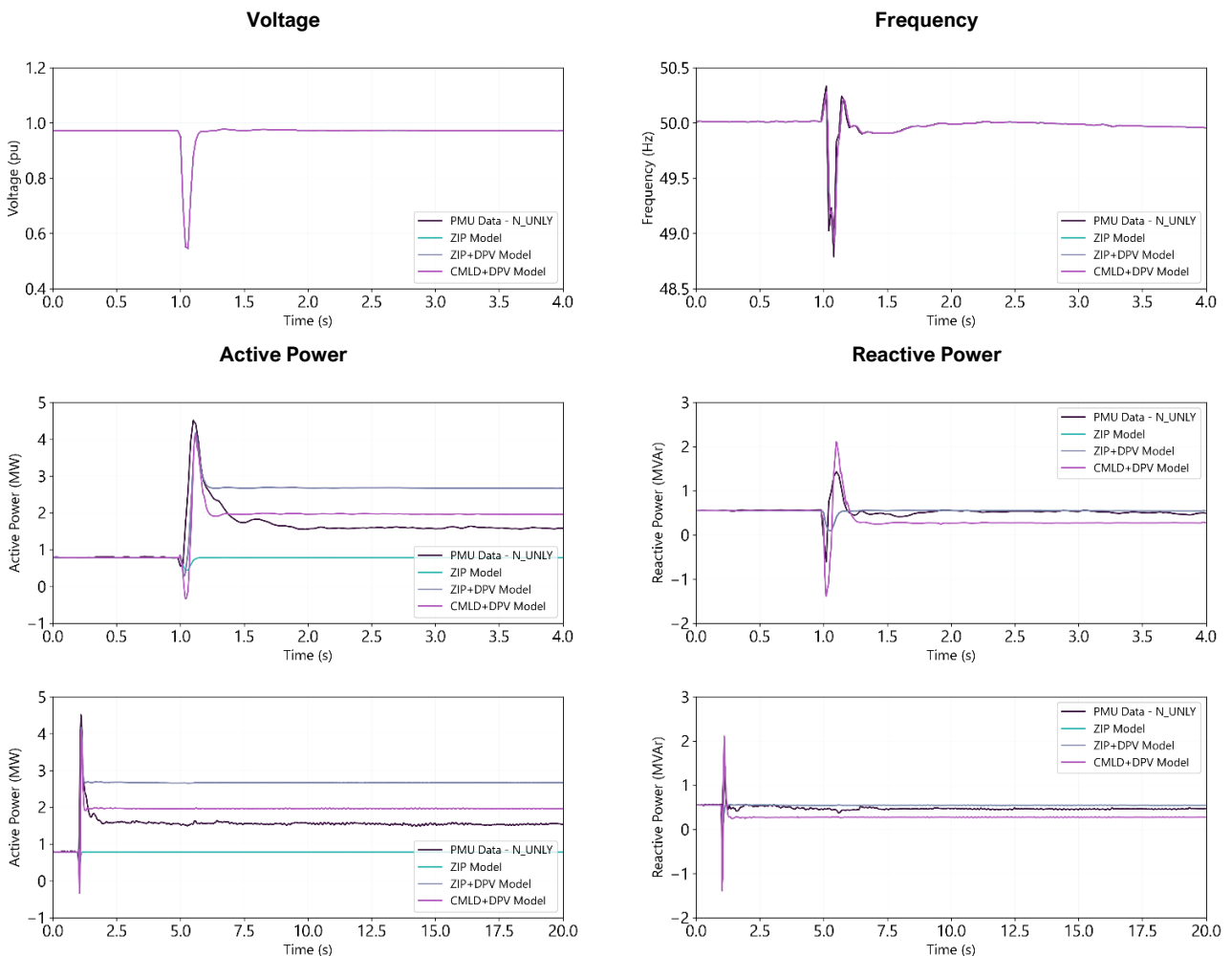
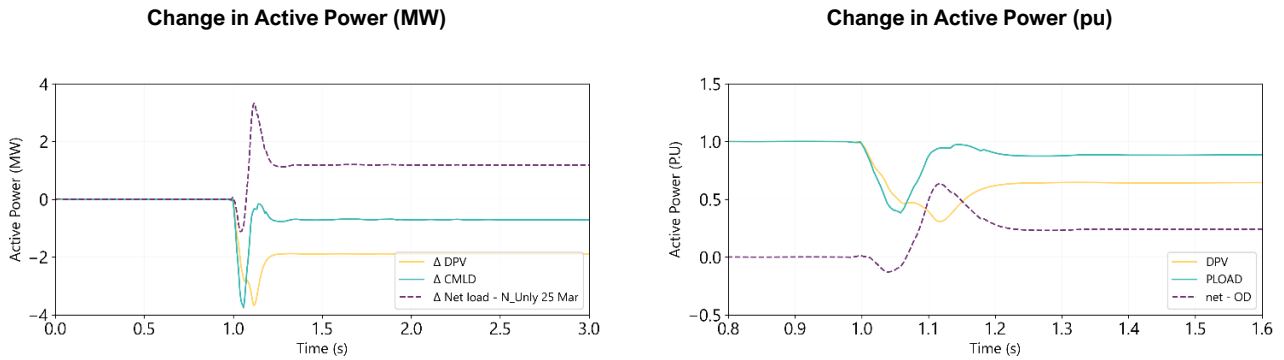


Figure 24 shows the individual responses of each of the CMLD and DPV models, as the change from a normalised pre-fault value. The DPV response is a significant contributing factor at this location. The active power of the CMLD model recovers post fault slightly more rapidly than the DPV model, which leads to a significant transient rise or “swing” in operational demand post fault. This swing persists until the system stabilises ~300ms after the fault. This behaviour has significant implications for power system stability and is discussed further in Section 6.1.

As shown in Figure 23, the CMLD+DPV models replicate the measured observations of active power very closely at this location (this swing in operational demand is observed in reality), suggesting this is accurately representing a real behaviour.

**Figure 24 Active power response of each model: 11kV North Unley (N\_UNLY)**

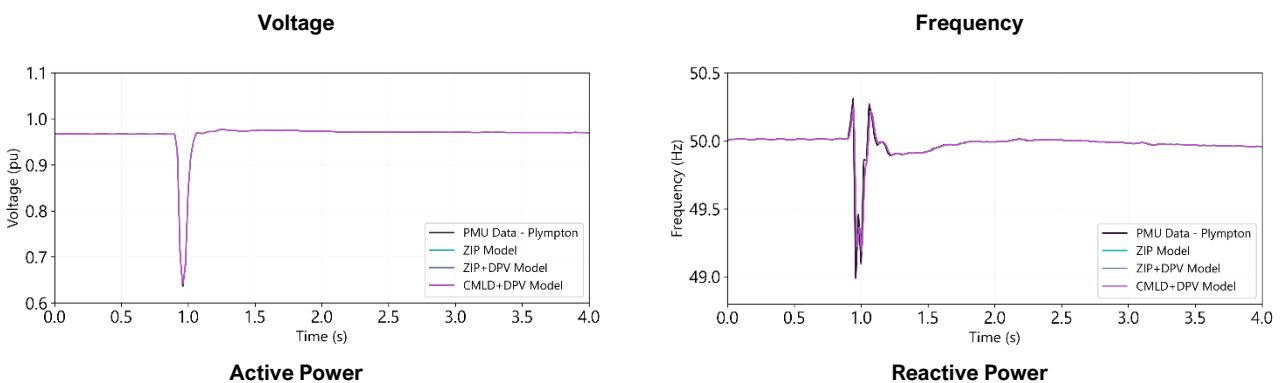


### 3.2.2 11 kV Plympton (PLYMPTON)

Figure 25 presents the simulation results for the 11 kV Plympton feeder in South Australia. Observations are similar to those for North Unley:

- Active Power:** At this location, DPV shake-off exceeds load shake-off, resulting in a net increase in measured active power post fault. This is well captured by the CMLD+DPV model, but not captured at all by the ZIP model. There is also clear evidence of a significant transient rise or “swing” in net measured demand post fault that is well captured by the CMLD+DPV model (and not captured at all by the ZIP model); this is discussed further below.
- Reactive Power:** The ZIP model doesn’t capture the transient dynamics at all, while the CMLD+DPV model provides an accurate representation of the transient rise in reactive power post fault. At this location, the steady state post fault reactive power is relatively unchanged from pre-fault levels and is well represented by both models.

**Figure 25 PMU data vs playback simulation results: 11KV Plympton (PLYMPTON)**



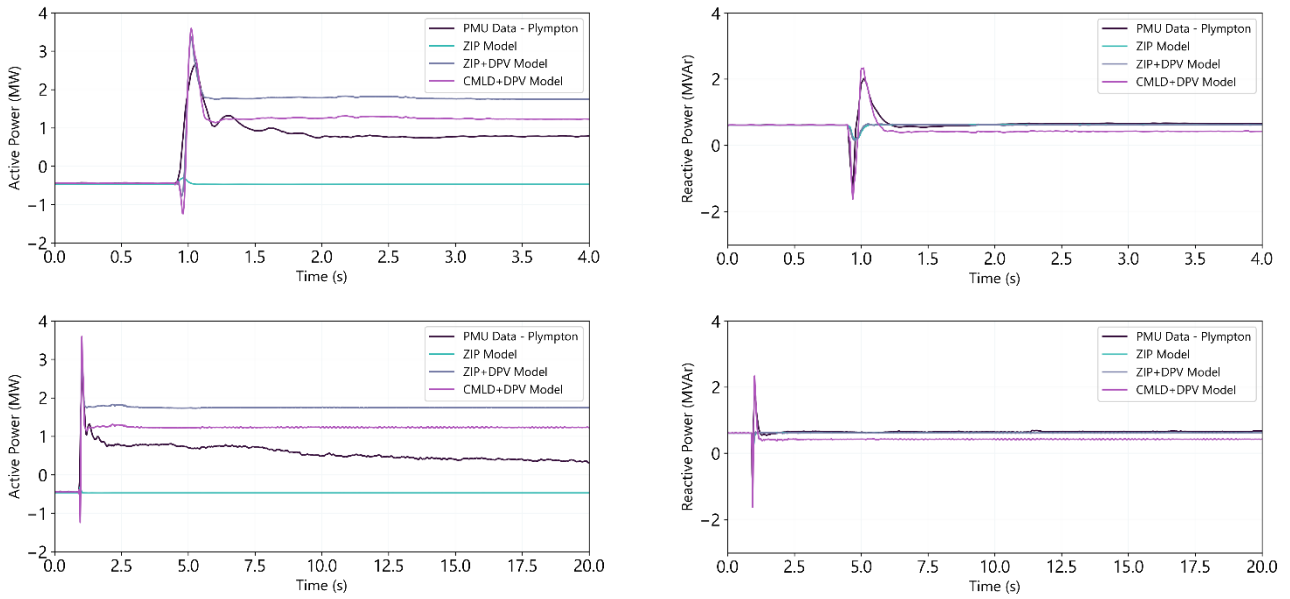
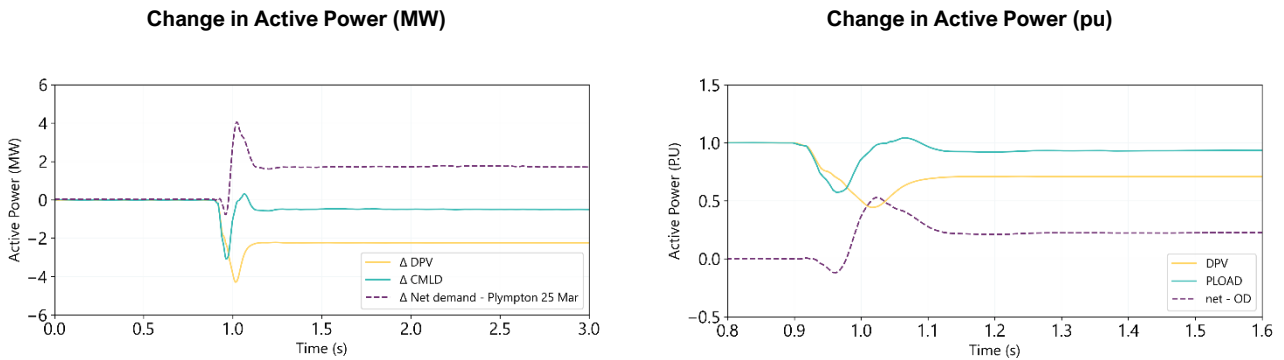


Figure 26 shows the contributions of the DPV and CMLD models to the modelled outcomes at this location. Both the CMLD and DPV models make a significant contribution. As observed for North Unley, the active power of the load model recovers slightly faster post fault than the DPV model, leading to a significant transient rise or “swing” in net demand post fault. This accurately reflects the measurements at this location (as shown in Figure 25), providing further validation that this is an accurate representation of a real behaviour observed in the field. This is discussed further in Section 6.1.

**Figure 26 Active power response of each model: 11kV Plympton (PLYMPTON)**



### 3.3 System-wide studies

#### 3.3.1 Replication in PSS®E

The following simulation was performed in PSS®E to replicate this case for system-wide studies:

**Table 8 Simulation event summary – 25 March 2024**

Time (s)	Events/comments
0.0	Start simulation.
1.0	Apply a 1PG fault on the 275 kV Torrens Island B Power Station bus (PSS®E bus 591080) <sup>17</sup>
1.0594 <sup>18</sup>	Clear the 1PG fault on the 275 kV Torrens Island B Power Station bus (PSS®E bus 591080) Trip TIPS B bus (PSS®E bus 591003) Trip TIPS B G3 generator (PSS®E machine 591003) Trip TIPS B G3 275/16 kV transformer (PSS®E bus 591003 to 591080) Trip TIPS B – LeFevre branch (PSS®E bus 591080 to 541580)
2.1994 <sup>19</sup>	Auto-reclose TIPS B – LeFevre branch (PSS®E bus 591080 to 541580) <sup>20</sup> .
60	End simulation.

### 3.3.2 High Speed Measurements

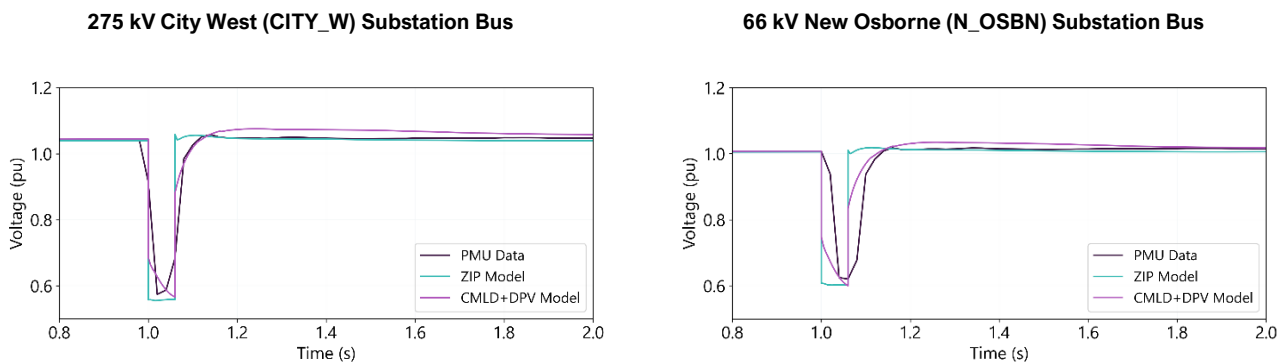
#### Voltages

Figure 27 shows the voltages recorded at several key locations close to the fault. Observations are as follows:

- The rate of voltage recovery is better represented by the CMLD model (the ZIP model recovers too quickly).
- Both models accurately represent that there is no voltage overshoot post fault.

Similar findings were also observed at 275 kV Para, Lefevre, and Barkers Inlet.

**Figure 27 Voltages – 25 March 2024**



#### Active and reactive power flows

Figure 28 shows the active and reactive power flow observations on the 275kV City West Power Station to Torrens Island B Power Station (TIPS B) feeder. The active power measurements at this location are poorly represented by all models although the CMLD+DPV models does capture the trajectory of the power flow. This misrepresentation

<sup>17</sup> The fault impedance was tuned to match the PMU data.

<sup>18</sup> According to PMU data from ElectraNet, the total fault clearing time was 59.4 ms.

<sup>19</sup> This is based on the time that the two 275 kV Circuit Breakers (CBs) at TIPS B (BE3) and Lefevre (6570) were in the open position, prior to auto-reclosing. Auto reclose occurred 1.14 s after the fault.

<sup>20</sup> Simulated the reclose of all three phases in PSS®E as individual phases cannot be closed independently.

is due to recloser operation on the TIPS B to Lefevre branch changing the magnitude of the active power flows within the 275 kV metro network which users are unable to instruct in PSS®E.

At this location, the CMLD + DPV and ZIP models overestimate peak reactive power flows, while both models reasonably replicate the overall trajectory of the reactive power profile during the dynamic and steady-state periods.

**Figure 28 Active/reactive power – 25 March 2024 – 275kV City West PS to TIPS B Feeder**

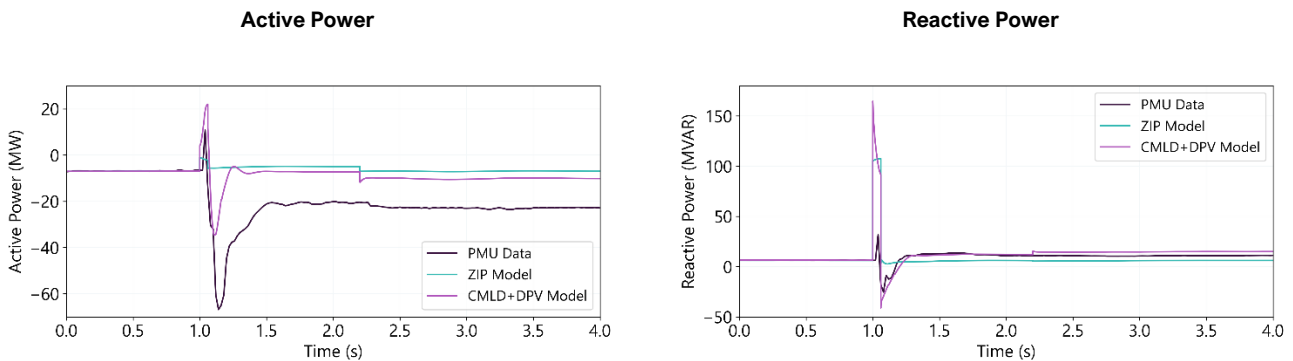
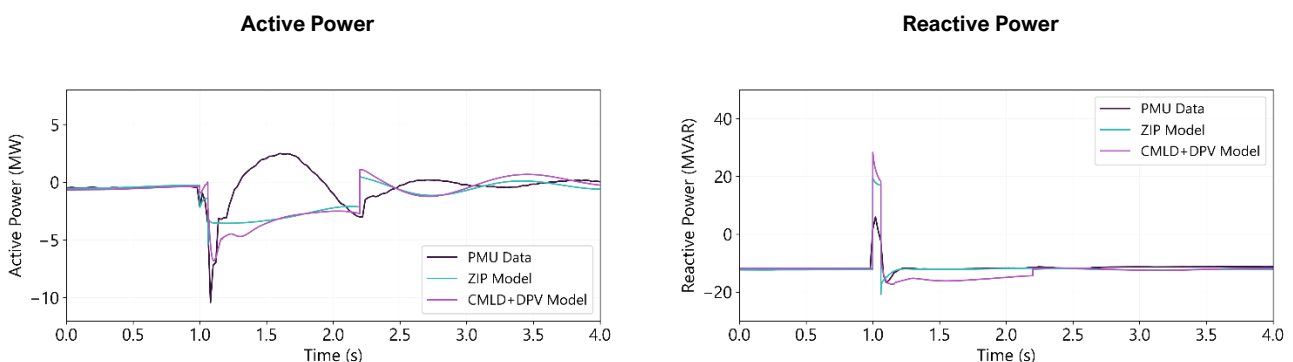
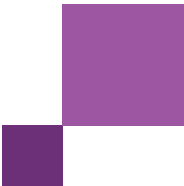


Figure 29 presents the active and reactive power flow observations on the 66kV Torrens Island A Power Station (TIPS A) to New Osborne Power Station feeder. Both CMLD + DPV and ZIP models underestimate the peak active power flows. During the fault, the active power in both models shows a step change and slightly deviates from the PMU trajectories corresponding to the operation of auto-reclosers on the nearby 275 kV LeFevre to TIPS B line. This discrepancy arises because single-phase auto-recloser operation occurred at the time of the event, which cannot be replicated in PSS®E. Instead, three-phase recloser operation needed to be simulated on the 275 kV line.

In this disturbance, the CMLD + DPV and ZIP models closely replicate the overall trajectory of the reactive power profile in the dynamic and steady state. However, both models overestimate peak reactive power flows.

**Figure 29 Active/reactive power – 25 March 2024 - 66 kV TIPS A to New Osborne PS Feeder**

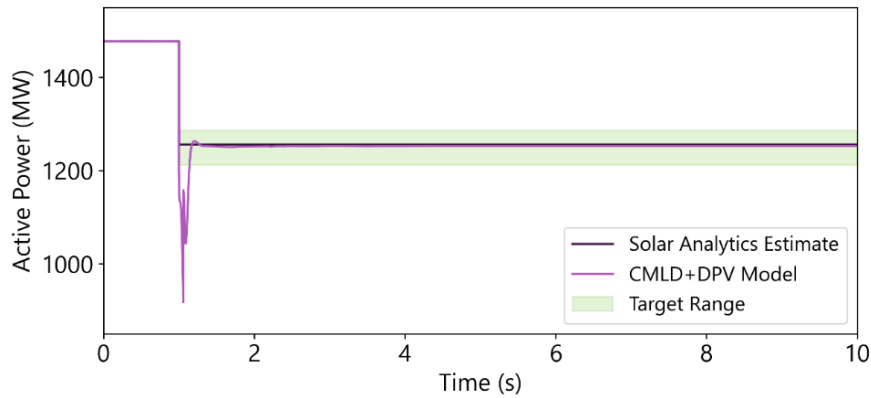




### 3.3.3 DPV shake-off

Figure 30 shows the total estimated change in DPV active power generation in South Australia<sup>21</sup> compared with the performance of the CMLD + DPV model. During the simulation, the model accurately predicts the 222 MW DPV disconnection estimated for this event.

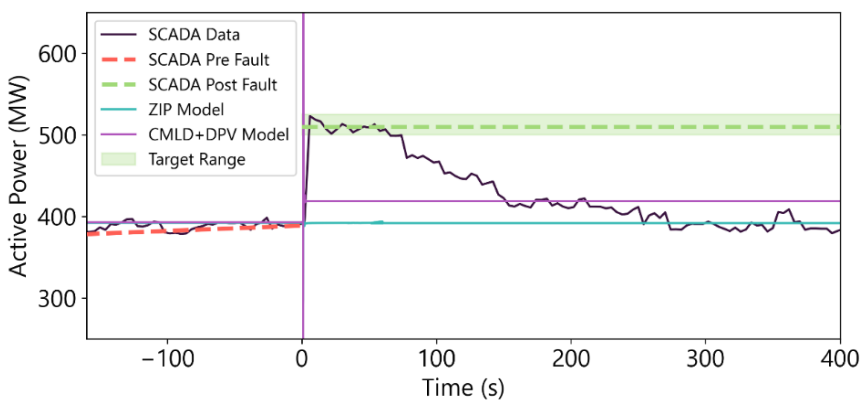
**Figure 30** DPV measurements – South Australia total – 25 March 2024



### 3.3.4 Load shake-off

Figure 31 shows the total measured operational demand from SCADA in South Australia, overlaid with the CMLD+DPV and ZIP model responses. Following the disturbance, operational demand briefly rose by roughly 118 MW (likely due to a greater disconnection of DPV than load), and then steadily declined to a minimum about six minutes later (not shown) as previously disconnected DPV systems and load reconnected. Because of significant uncertainties in the SCADA measurements, the CMLD+DPV model was tuned to match the average load change at around 60 seconds post-disturbance (indicated by the green dashed line), with the green “target range” depicting a margin of measurement error.

**Figure 31** Operational demand measurements (SCADA) – 25 March 2024



<sup>21</sup> The initial value is estimated from a combination of Rooftop PV (from ASEFS2) and PVNSG (from LRET), while the post-disturbance change is estimated using Solar Analytics datasets, with both estimates considering interpolation.

As Figure 31 illustrates, the CMLD+DPV model underestimates the observed 118 MW increase in operational demand. The model predicts a total underlying load loss of 200 MW, which is offset by an estimated 224 MW of DPV disconnection, leading to a net rise of just 24 MW. Table 9 summarises this discrepancy.

**Table 9 Summary of change in demand and distributed PV – 25 March 2024**

	Actuals (estimated)	CMLD + DPV prediction
<b>Change in distributed PV generation (estimated from Solar Analytics sample)</b>	222 MW (192 – 266 MW) decrease	223 MW decrease (accurate and within range)
<b>Change in underlying demand (estimated from SCADA &amp; Solar Analytics)</b>	104 MW (59 – 158 MW) decrease	200 MW decrease (overestimates by 95 MW)
<b>Change in operational demand (estimated from SCADA, 60s post disturbance)</b>	118 MW (108 – 133 MW) increase	23 MW increase (underestimates by 95 MW)

Because the ZIP model does not account for any load disconnection, it cannot replicate the observed net demand changes. Despite not fully matching the measured range, the CMLD+DPV model still offers an improvement over the ZIP model.

### 3.3.5 Summary of model performance in system wide studies

Table 10 provides a summary of the model performance for this event.

**Table 10 Assessment of model performance – 25 March 2024**

Quantity	Characteristic	CMLD + DPV estimates	CMLD + DPV model equal (✓) or better (✓✓) than ZIP?	Commentary
<b>Voltages</b>	Voltage overshoot	Good match	✓	The CMLD + DPV accurately represents peak voltage overshoot and stays within the normal voltage range as defined in the NER (0.9 to 1.1 pu).
	Voltage recovery rate	Good match	✓✓	CMLD + DPV aligned with PMU.
	Steady-state post disturbance	Good match	✓	CMLD + DPV voltages are accurate (settles to within 5% of the PMU data for all voltage channels).
<b>Active power</b>	During dynamic state	Fair match	✓✓	CMLD + DPV trajectory aligned with PMU data but underestimates the minimum flows during the fault. This is due to auto-recloser operation and swings in active power flows on the 275 kV metro network which is difficult to represent in PSS®E.
	Steady-state post disturbance	Fair match	✓	CMLD + DPV underestimates the steady-state active power magnitude.
<b>Reactive power</b>	During dynamic state	Fair match	✓	CMLD + DPV trajectory aligned with PMU data but significantly overestimates the peak reactive power during the fault.
	Steady-state post disturbance	Good match	✓	CMLD + DPV aligned with PMU.
<b>DPV</b>	DPV change	Good match	✓✓	Estimated actuals: 222 MW decrease DPV: 223 MW decrease The DPV model accurately estimates DPV disconnection.
<b>CMLD</b>	Underlying load change	Fair match	✓✓	Estimated actuals: 104 MW decrease, 6% reduction from pre-fault condition. CMLD: 200 MW decrease, 11% reduction from pre-fault condition. CMLD overestimates load disconnection by 96 MW.
<b>Operational Demand</b>	Net load change	Poor match	✓✓	Estimated actuals: 118MW increase CMLD + DPV: 23 MW increase The CMLD + DPV model underestimates net load change by 95MW.

## 4 South Australia: 27 March 2024

### 4.1 Event overview

On 27 March 2024, Torrens Island Power Station A (TIPS A) experienced a trip involving the 275 kV West busbar and circuit breaker AC3. Subsequently, the 275 kV network at Para recorded a minimum positive sequence voltage of 0.6 pu. In response, the South Australian region saw a net load increase of approximately 68 MW, attributed to the shake-off of distributed photovoltaic (DPV) generation.

<30 kW inverters installed after April 2023 experienced minimal shake-off, while inverters sized 30–100 kW showed a 40% reduction in output regardless of installation date. Further details are available in the incident report<sup>22</sup> and its addendum<sup>23</sup>.

**Table 11** Event summary – 27 March 2024

<b>Date and time</b>		27 March 2024, 15:29 <sup>24</sup>
<b>Region</b>		South Australia
<b>Description of the event</b>		An internal fault in the 'U' phase CT occurred at the Torrens Island A substation at 15:29. The event is summarised as: <ul style="list-style-type: none"> <li>• Trip of TIPS A 275kV West busbar</li> <li>• Trip of TIPS A 275kV CB AC3, AW1, AW2, AW3, AW4, AWT, AWB</li> </ul> Fault cleared by tripping of protection systems.
<b>Minimum voltage recorded</b>		0.6pu positive sequence recorded at Para 275 kV
<b>Installed capacity of DPV</b>		Total installed capacity in South Australia: 2,780 MW <ul style="list-style-type: none"> <li>• 25% installed under AS4777.3:2005</li> <li>• 64% installed under AS4777.2:2015</li> <li>• 11% installed under AS4777.2:2020</li> </ul>
<b>Prior to the event</b>	<b>DPV</b>	1,298 MW, 47% capacity factor <ul style="list-style-type: none"> <li>• Rooftop PVs: 1,130 MW</li> <li>• PVNSGs: 168 MW</li> </ul>
	<b>Operational demand</b>	589 MW
	<b>Underlying demand</b>	1,887 MW
<b>Estimated change (post disturbance vs pre disturbance)</b>	<b>DPV</b>	143 MW (range of 117-156 MW) decrease
	<b>Operational demand</b>	68 MW (range of 61-81 MW) increase
	<b>Underlying demand</b>	75 MW (range of 36-95 MW) decrease

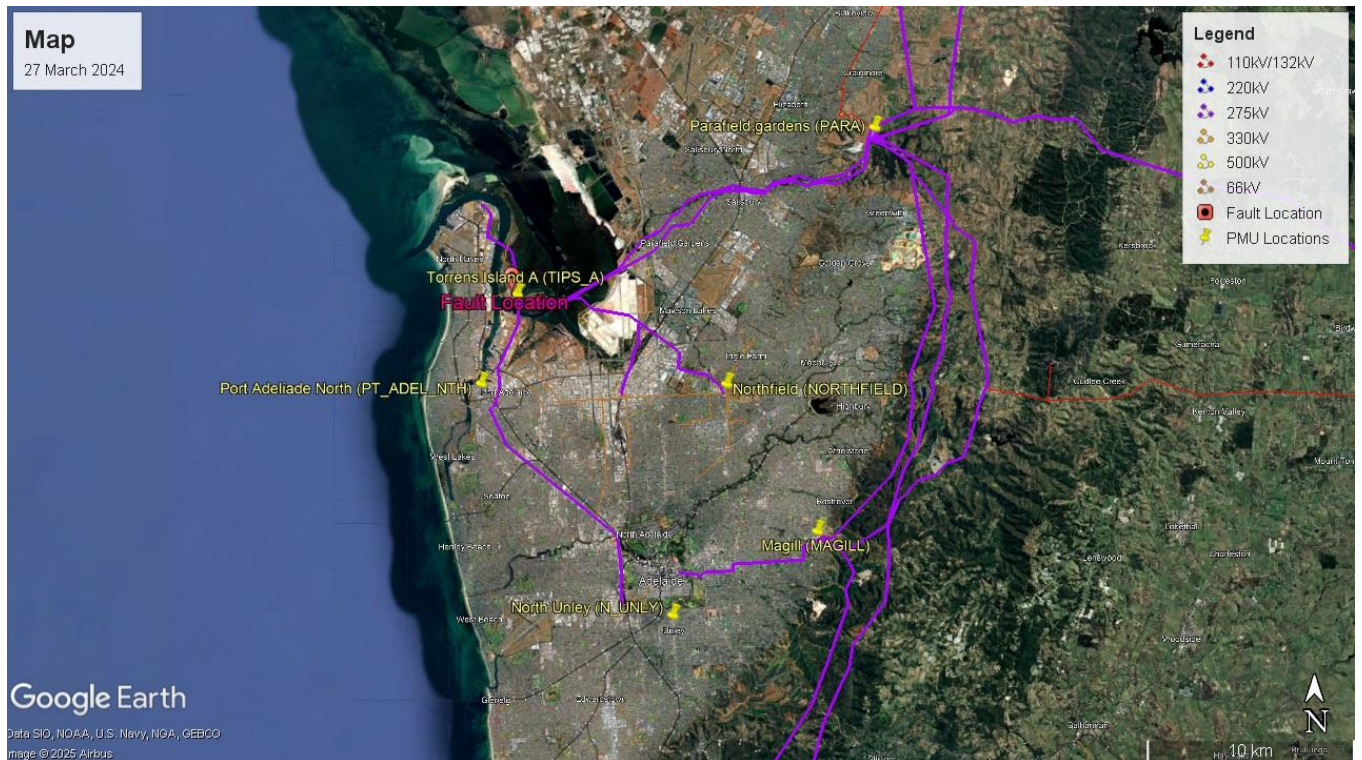
<sup>22</sup> AEMO (September 2024) 275kV current transformer failures in South Australia 14-27 March, [https://aemo.com.au/-/media/files/electricity/nem/market\\_notices\\_and\\_events/power\\_system\\_incident\\_reports/2024/report-on-current-transformer-failures-during-march-2024-in-south-australia.pdf?la=en&hash=E0EE498E5BBDBF24F0CCA7CEE4E7EE08](https://aemo.com.au/-/media/files/electricity/nem/market_notices_and_events/power_system_incident_reports/2024/report-on-current-transformer-failures-during-march-2024-in-south-australia.pdf?la=en&hash=E0EE498E5BBDBF24F0CCA7CEE4E7EE08)

<sup>23</sup> AEMO (October 2024) Addendum on DPV and load behaviour: 275kV current transformer failures in South Australia 14-27 March 2024, [https://aemo.com.au/-/media/files/electricity/nem/market\\_notices\\_and\\_events/power\\_system\\_incident\\_reports/2024/addendum-on-dpv-and-load-behaviour275-kv-current-transformer-failures-in-south-australia-1427-march.pdf](https://aemo.com.au/-/media/files/electricity/nem/market_notices_and_events/power_system_incident_reports/2024/addendum-on-dpv-and-load-behaviour275-kv-current-transformer-failures-in-south-australia-1427-march.pdf)

<sup>24</sup> AEMO. Fault at Torrens Island Switchyard and Loss of Multiple Generating Units on 3 March 2017, March 2017, at [https://aemo.com.au/-/media/files/electricity/nem/market\\_notices\\_and\\_events/power\\_system\\_incident\\_reports/2024/report-on-current-transformer-failures-during-march-2024-in-south-australia.pdf?](https://aemo.com.au/-/media/files/electricity/nem/market_notices_and_events/power_system_incident_reports/2024/report-on-current-transformer-failures-during-march-2024-in-south-australia.pdf?)

Figure 32 shows a map, indicating the location of the disturbance (Torrens Island Power Station A), and the locations where high-speed data measurements were available<sup>25</sup>.

**Figure 32** Map – 27 March 2024



## 4.2 Radial measurements (Single Load Infinite Bus simulations)

For this event, it was only possible to obtain radial data from one location: North Unley. Details are provided in Table 12. It is estimated that 4.6 MW of DPV was generating on this feeder at the time of this disturbance, contributing 65% of underlying demand.

**Table 12** Terminal station summary of voltage sag, DPV participation and end-use load type

Terminal Station	End-Use Load Type	Pre-Fault Active Power (MW)	DPV Generation (MW)	DPV contribution to underlying demand (%)	Minimum voltage recorded (pu)
11kV North Unley	Predominantly residential	2.45	4.6	65%	0.65

### 4.2.1 11 kV North Unley (N\_UNLY)

Figure 33 shows the comparison of the measurements at North Unley for this event with the performance of the various models. Observations are as follows:

<sup>25</sup> HSM data is available at 275 kV Northfield, 275 kV Magill, 275 kV Parafield Gardens, 275 kV Port Adelaide North, and 11 kV North Unley

- Active Power:** The measured data shows a small increase in active power post fault, indicating DPV shake-off exceeded load shake-off. This is best represented by the CMLD+DPV model. The ZIP model does not represent any change in active power, and the ZIP+DPV model exaggerates this effect significantly beyond observations (highlighting the importance of applying the CMLD model when using the DPV model). A significant transient rise or “swing” in active power is observed post fault, and this is well captured by the CMLD+DPV models.
- Reactive Power:** The CMLD+DPV models capture the transient dynamics well, while the ZIP model fails to represent the observed dynamics.

**Figure 33** PMU data vs playback simulation results: 11kV North Unley (N\_UNLY)

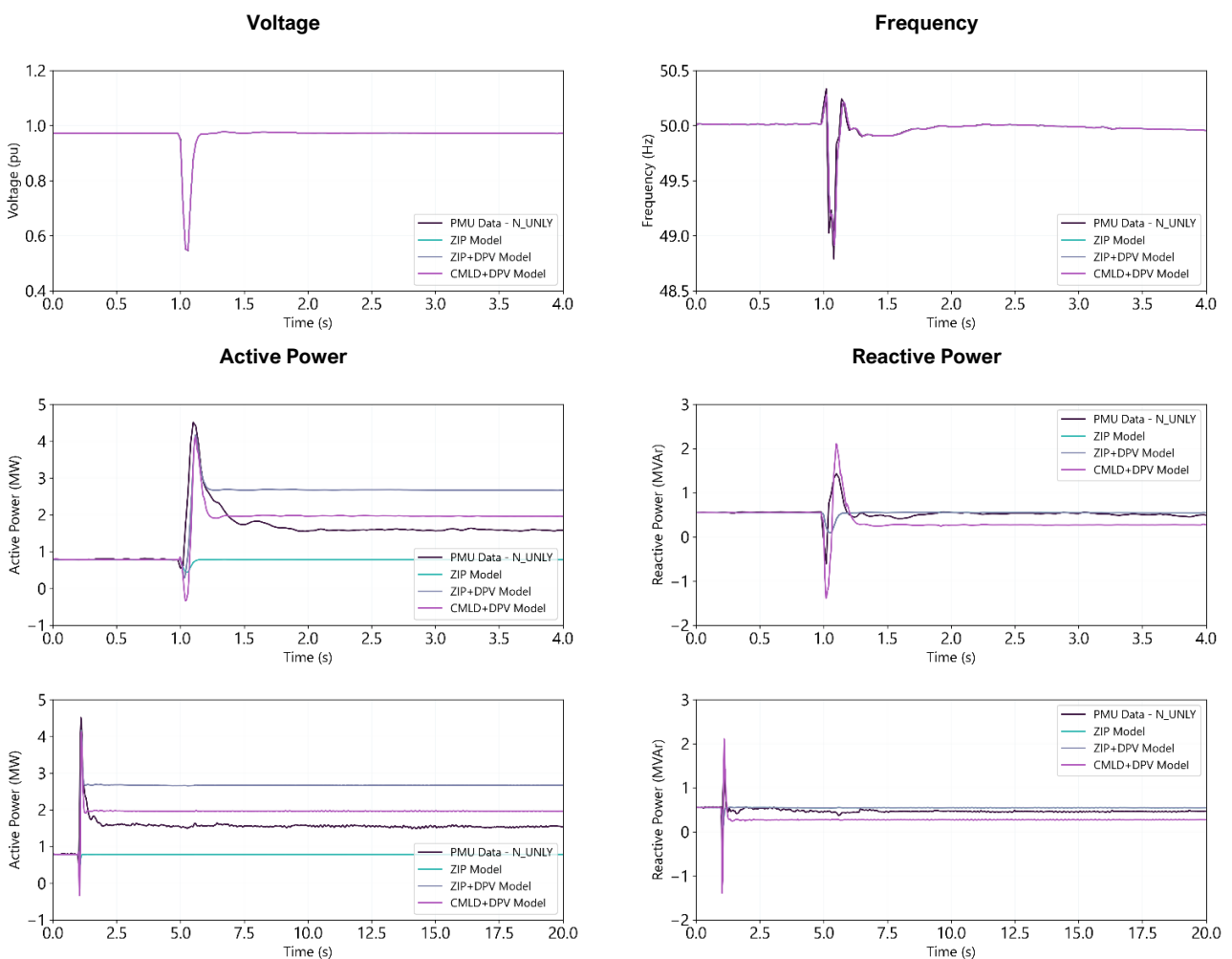
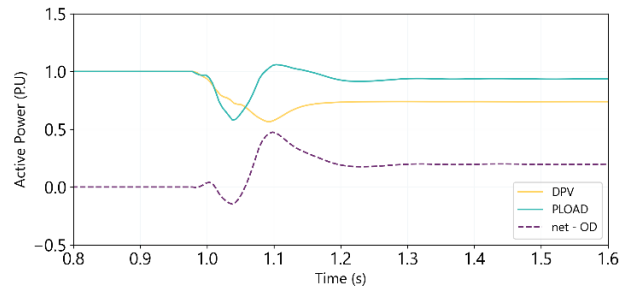
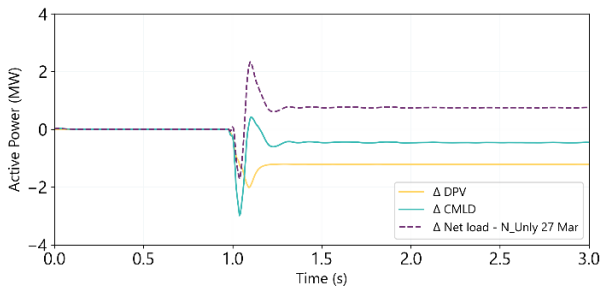


Figure 34 shows the contributions of each of the CMLD and DPV models separately to these active power behaviours. Both are significant contributors at this location. The transient rise or “swing” post fault (accurately replicating observed measurements) is due to the CMLD model recovering more quickly than the DPV model post fault; this is discussed further in Section 6.1.

**Figure 34** Active power response of each model: 11kV North Unley (N\_UNLY)

Change in Active Power (MW) Change in Active Power (pu)



### 4.3 System wide studies

#### 4.3.1 Replication in PSS®E

The following element changes were made in PSS®E to replicate this case:

**Table 13** Simulation event summary – 27 March 2024

Time (s)	Events/comments
0.0	Start the simulation.
1.00	Apply a 1PG fault on the 275 kV Torrens Island A Power Station bus (PSS®E bus 590580) <sup>26</sup> .
1.0507	Clear the 1PG fault on the 275 kV Torrens Island A Power Station bus (PSS®E bus 590580).
60.00	End simulation.

#### 4.3.2 High speed measurements

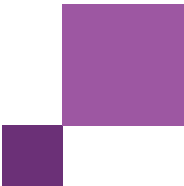
##### Voltages

Figure 35 shows voltages measured at several key locations<sup>27</sup>. Observations are as follows:

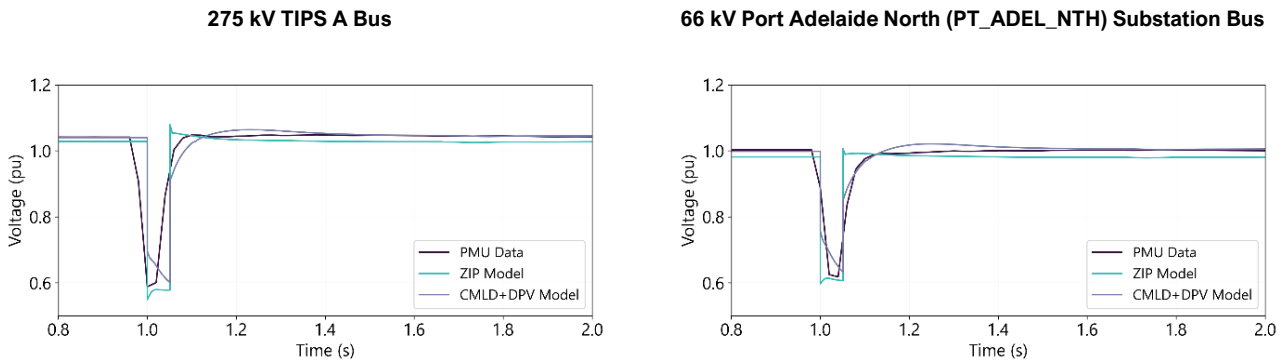
- The CMLD+DPV model closely matches the measured recovery, offering a clear improvement over the ZIP model (which returns to nominal voltage too rapidly).
- The ZIP model shows a slight overshoot (within the 0.9–1.1 pu. range). The CMLD+DPV model avoids this overshoot, reducing the risk of inadvertent protection trips in PSS®E simulations.

<sup>26</sup> No lines or generation tripped for this event. The busbar trip was not modelled as it makes no difference to the outcome of the simulation.

<sup>27</sup> PMU data from ElectraNet was available at the following locations: 275kV TIPS B to Lefevre Feeder and Barkers Inlet Feeder, 275kV City West Bus, 275kV City West to TIPS B Feeder, 275kV Cherry Gardens to Happy Valley Feeder and TIPS B Feeder, 275kV Northfield to Kilburn Feeder, as well as 66kV TIPS A to Torrens Island North Feeders and New Osborne Feeders.



**Figure 35** Voltages – 27 March 2024



Observations were similar at other monitored locations.

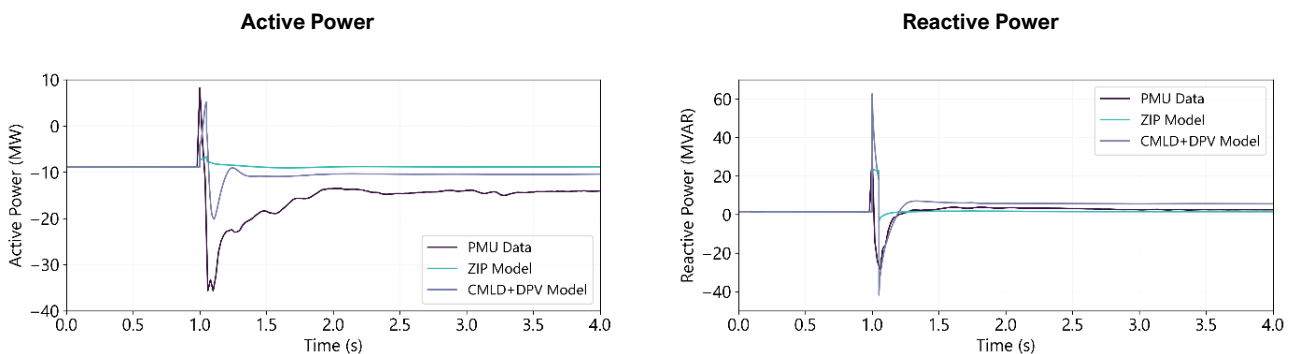
### Active and reactive power flows

Figure 36 and Figure 37 shows active and reactive power measurements for several locations close to the fault. These measurements reflect typical power profiles at their respective voltage levels across the network.

Observations include:

- **Active Power:**
  - The measured data shows a significant drop in active power post fault. This is somewhat captured by the CMLD+DPV model but underestimated in magnitude.
- **Reactive Power:**
  - At the 275kV Northfield location, the CMLD+DPV models show an improved representation of the transient trajectory.
  - At the 66 kV Port Adelaide North location, both models follow the overall shape of the observed data but underestimate steady-state reactive power flows.

**Figure 36** Active/reactive power – 27 March 2024 – 275kV Northfield to TIPS A Feeder



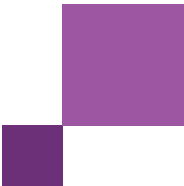
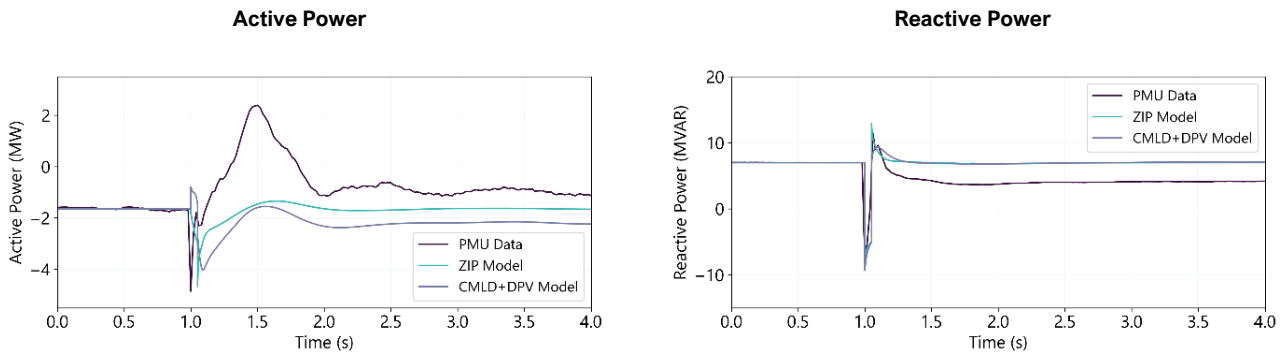


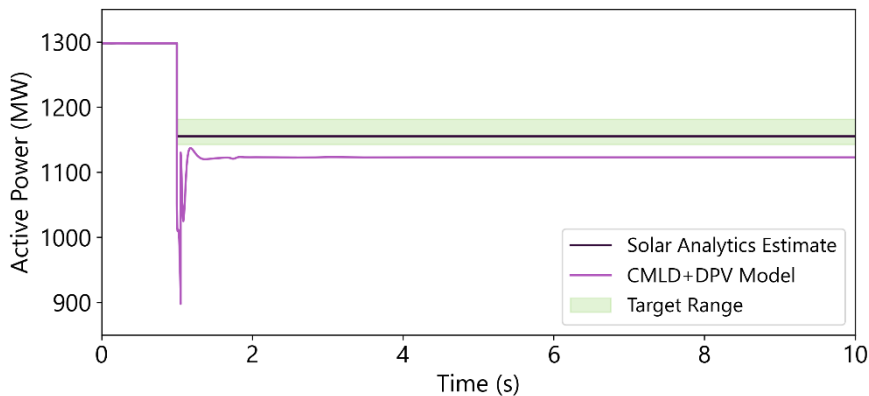
**Figure 37 Active/reactive power – 27 March 2024 – 66kV TIPS A to Port Adelaide North Substation Feeder**



### 4.3.3 DPV shake-off

Figure 38 shows the total estimated change in DPV generation in South Australia compared with the performance of the CMLD+DPV model. The DPV model somewhat overestimates the 143MW of DPV shake-off estimated for this event.

**Figure 38 DPV measurements – South Australia total – 27 March 2024**



### 4.3.4 Load shake-off

Figure 39 presents the SCADA-measured operational demand in South Australia alongside the CMLD+DPV and ZIP model outputs. During this event, operational demand rose (likely due to more rooftop PV systems tripping than loads) and then returned to pre-fault levels within about six minutes. The target range was defined as the average load change observed at 60 seconds post-disturbance (the green dashed line in Figure 39), acknowledging known SCADA inaccuracies.

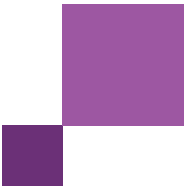
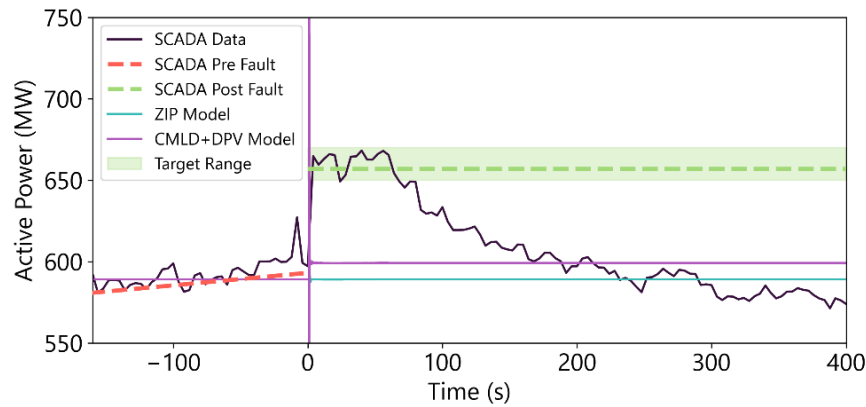


**Figure 39** Operational demand measurements (SCADA) – 27 March 2024



As seen in Figure 39, the CMLD+DPV model slightly underestimates the net 68 MW rise in operational demand. It predicts 165 MW of underlying load loss, offset by 175 MW of DPV disconnection, yielding a 10 MW net increase. Table 14 compares this outcome with estimated actuals, indicating that an overestimation of load loss is the principal cause of the overall error in net operational demand.

**Table 14** Summary of change in demand and distributed PV – 27 March 2024

	Actuals (estimated)	CMLD + DPV prediction
<b>Change in distributed PV generation (estimated from Solar Analytics sample)</b>	143 MW (117 – 156 MW) decrease	175 MW decrease (overestimates by 32 MW)
<b>Change in underlying demand (estimated from SCADA &amp; Solar Analytics)</b>	75 MW (36 – 95 MW) decrease	165 MW decrease (overestimates by 90 MW)
<b>Change in operational demand (estimated from SCADA, 60s post disturbance)</b>	68 MW (61 – 81 MW) increase	10 MW increase (underestimates by 58 MW)

In contrast, the ZIP model cannot represent any load disconnection.

### 4.3.5 Summary of model performance in system wide studies

Table 15 provides a summary of the model performance for this event.

**Table 15 Assessment of model performance – 27 March 2024**

Quantity	Characteristic	CMLD + DPV estimates	CMLD + DPV model equal (✓) or better (✓✓) than ZIP?	Commentary
<b>Voltages</b>	Voltage overshoot	Good match	✓	CMLD + DPV accurately represents peak voltage overshoot and stays within the normal voltage range as defined in the NER (0.9 to 1.1 pu).
	Voltage recovery rate	Good match	✓✓	CMLD + DPV comparable to PMU.
	Steady-state post disturbance	Good match	✓	CMLD + DPV voltages are accurate (settles to within 5% of the PMU data for all channels).
<b>Active power</b>	During dynamic state	Fair match	✓✓	CMLD + DPV has a similar trajectory to the PMU, although it underestimates peak flows during the fault.
	Steady-state post disturbance	Fair match	✓	CMLD + DPV slightly underestimates the net load change on the feeders.
<b>Reactive power</b>	During dynamic state	Fair match	✓✓	CMLD + DPV trajectory aligned with PMU data for all channels, although peak flows are overestimated in some cases.
	Steady-state post disturbance	Good match	✓	CMLD + DPV aligned with PMU.
<b>DPV</b>	DPV change	Fair match	✓✓	Estimated actuals: 143 MW decrease DPV: 175 MW decrease The DPV model overestimates DPV disconnection by 32 MW.
<b>CMLD</b>	Underlying load change	Fair match	✓	Estimated actuals: 75 MW decrease, 4% reduction from pre-fault levels. CMLD: 165 MW decrease, 9% reduction from pre-fault levels.
<b>Operational Demand</b>	Net load change	Fair match	✓	Estimated actuals: 68 MW increase CMLD + DPV: 10 MW increase

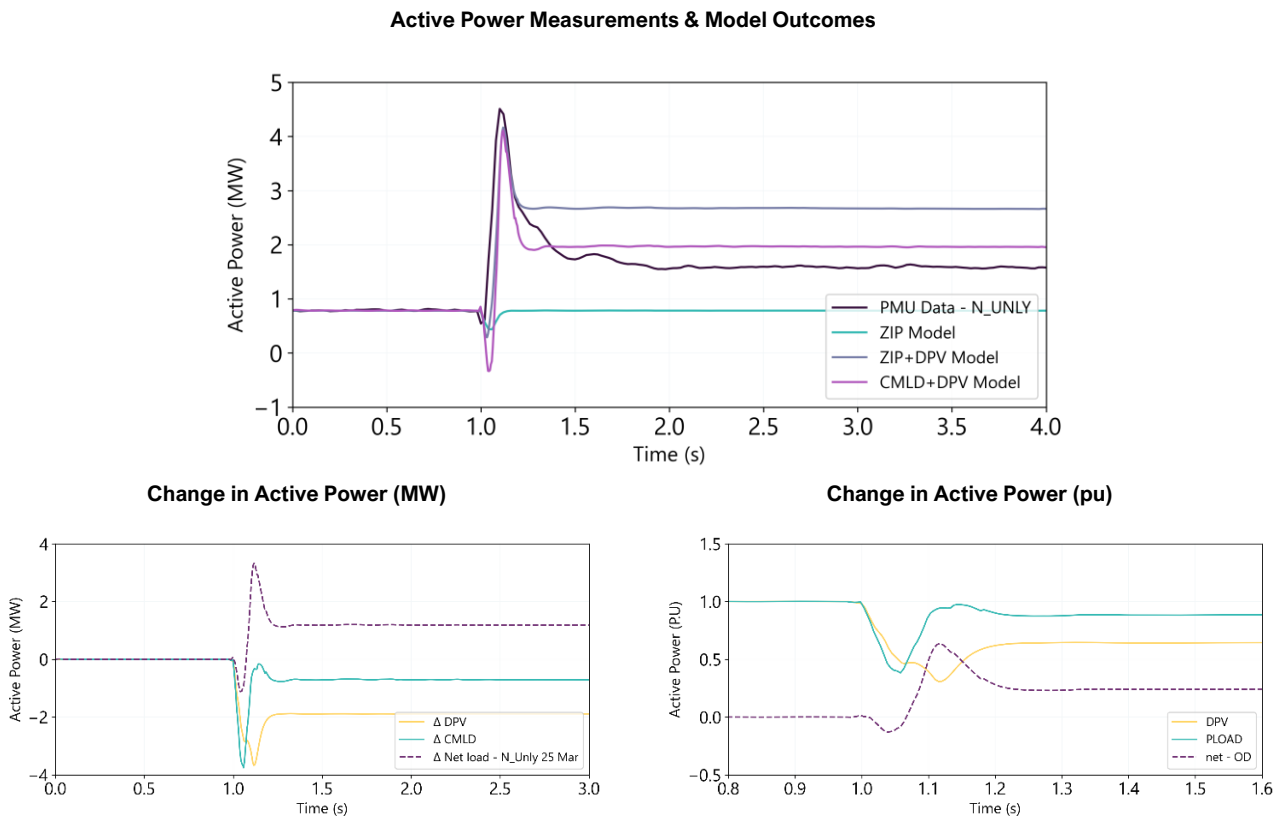
## 5 Operational Demand Swings

As noted in Section 3.2 and 4.2, in scenarios where DPV is contributing a high proportion of underlying load, the radial measurements show a significant transient rise or “swing” in operational demand post fault. This swing persists until the system stabilises ~300ms after the fault. An example is shown in Figure 40. This behaviour can have significant implications for power system stability in cases with a significant proportion of underlying demand met by distributed PV and is therefore discussed in more detail in this section.

This behaviour is well replicated by the CMLD+DPV models. It arises due to the CMLD model recovering more quickly post fault, while the DPV model takes slightly longer to recover (as shown in the lower panels in Figure 40). This leads to a transient increase in operational demand. This transient swing can be very significant in cases where the DPV is supplying a significant proportion of underlying demand pre fault (explored further below).

As shown in Figure 40 (and the other figures in Section 3.2 and 4.2) the CMLD+DPV models consistently replicate these measured observations of active power well (this swing in operational demand is observed in reality), suggesting the models are accurately representing a real behaviour.

**Figure 40** North Unley – 25 March 2024 – Playback simulation



## 5.1 Influence of DPV levels on operational demand swings

Figure 41 shows high speed data measured at radial locations in the South Australian network for the disturbances on 25 and 27 March 2024. The measurements have been normalised to per unit values, based on the pre-fault operational demand. The figure shows that:

- The swing in operational demand post fault is consistently observed
- The size of the swing appears to be strongly affected by the contribution of DPV (indicated as a percentage of contribution to underlying demand at the feeder), and likely also by the depth of the fault measured at each location.

**Figure 41** Swings in operational demand captured by measurements in different locations

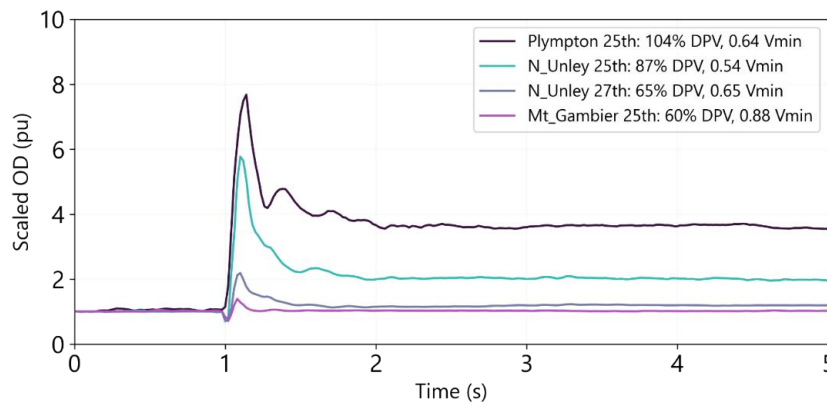


Table 16 quantifies the magnitude of the operational demand swings (as a percentage of pre-fault operational demand). The data indicates that higher DPV shares are associated with more pronounced swings in operational demand.

**Table 16** Operational Demand swings captured from PMU data for 25 March and 27 March events in SA

Terminal Station	Pre-fault operational demand (MW)	DPV % contribution to underlying demand	Magnitude of operational demand swing (MW)	Magnitude of operational demand swing (% of pre-fault operational demand)
11 kV North Unley, 27 March	2.45	65%	5.4	218%
11 kV North Unley, 25 March	0.78	87%	4.5	576%
11 kV Plympton, 25 March	-0.47	104%	2.7	768%

## 5.2 Regional level implications

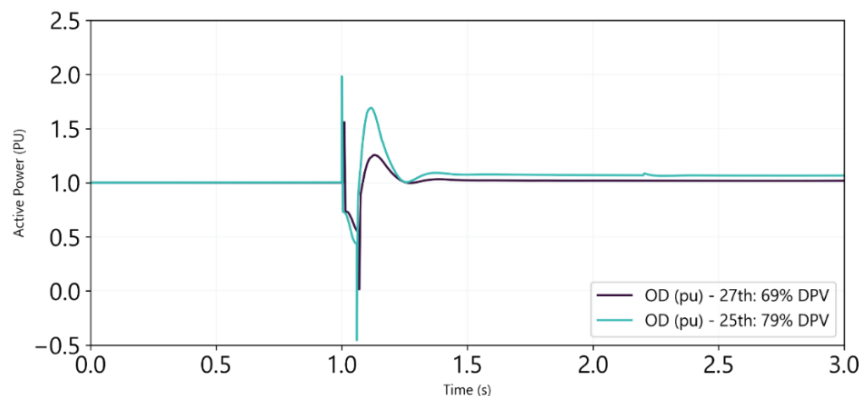
The measurements above are for selected radial loads. Since the regional operational demand is effectively the sum of operational (net) demand at the substation level (comprising measurable loads observed from distribution substations and associated power losses), simulating faults at the South Australian level can provide an estimate of operational demand swings for the entire region. Different loads within the system have varying levels of DPV

contribution, and experience different voltage depression levels during disturbances, and therefore will demonstrate this operational demand swing behaviour to different degrees.

Figure 42 shows the total South Australian operational demand (normalised to pre-event operational demand) for the 27 March 2024 event, as simulated by the CMLD+DPV models. On 27 March, DPV was supplying 69% of underlying demand in South Australia. The simulation for these conditions suggests that the operational demand swing can be observed on a region-wide basis (although it is less pronounced across the whole region compared with selected radial load feeders that have high DPV generation levels close to the fault location).

As also shown in Figure 42, the normalised total South Australian operational demand for the 25 March 2024 event, where DPV-generated power was supplying 79% of the total regional underlying demand. The simulation results for this case, that compares 25<sup>th</sup> of March scenario with 79% DPV to 27<sup>th</sup> of March scenario with 69% DPV, indicates that increasing the total DPV generation results in a significantly larger swing in operational demand<sup>28</sup>. This phenomenon arises because higher DPV generation results in a larger deficit in active power when the DPV model recovers more slowly than the CMLD model following a fault. This implies that higher levels of DPV generation lead to more pronounced swings in operational demand.

**Figure 42 Simulated South Australian total regional operational demand (pu): 25 and 27 March**



No whole-region high speed measurements are available to validate these whole-region effects; they are estimated as an extrapolation of application of the model to the entire region. However, the validation of these model effects based on radial load measurements suggests that this behaviour is likely a real representation of power system outcomes.

### 5.3 Impact of fault severity and DPV penetration on operational demand swings

Figure 43 compares simulation results for a number of sensitivities, based on the 27 March South Australian event as a base case. The studies vary the DPV generation levels (maintaining the underlying demand level constant)<sup>29</sup>. The severity of the fault was also varied, replacing the original fault with a more severe fault occurring at the

<sup>28</sup> The underlying demand, operational demand, and total DPV in MW for these two cases are given in section 2.1 and 3.1.

<sup>29</sup> An increase in DPV generation in the case was offset by an equivalent power transfer from SA to VIC over the Heywood interconnector.

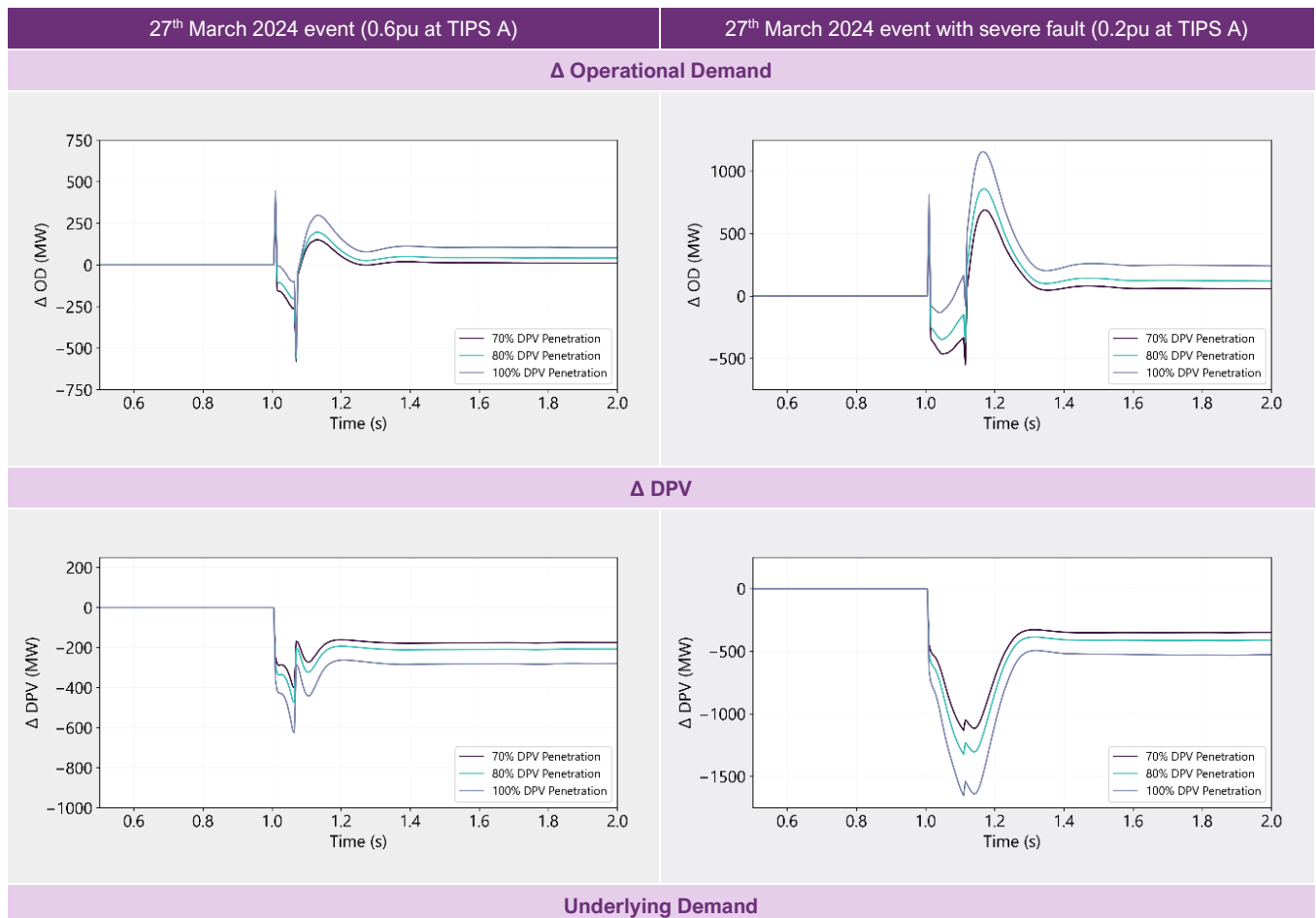
Torrens Island Power Station (TIPS) A bus (a two-phase-to-ground (2PG) fault with a duration of 100 ms, representing a credible, high-impact scenario).

Observations include:

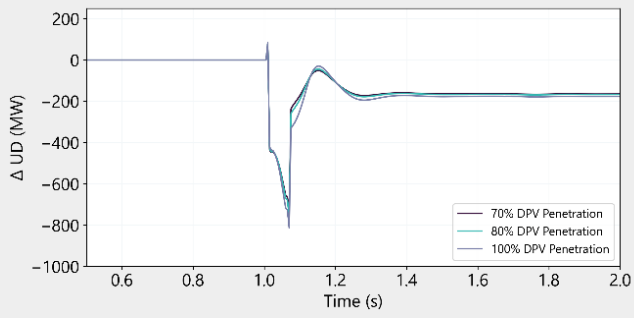
- The size of the operational demand swing grows larger as the contribution of DPV to underlying demand increases.
- The more severe fault also exacerbates the size of the operational demand swing.
- The total size of the operational demand swing can exceed 1000 MW for up to 200ms (for the case of a severe but credible fault, in the South Australian network with DPV contributing 100% of operational demand).

These results suggest that this effect could become increasingly influential in defining power system secure limits as levels of DPV grow. This increases the importance of applying the CMLD+DPV models (or other models that accurately represent these effects), since these effects are not captured by the traditional ZIP modelling approach.

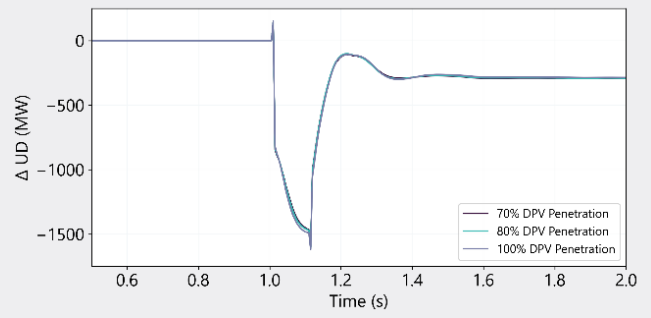
**Figure 43** Impact of fault severity and DPV penetration on operational demand swings



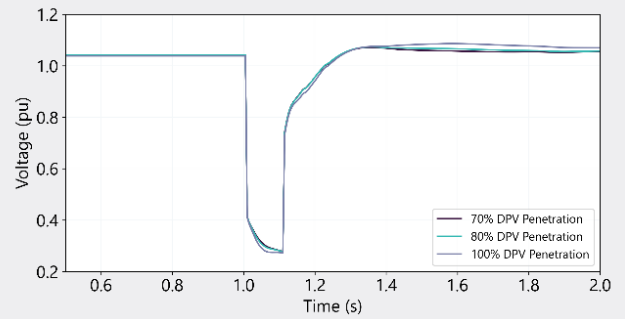
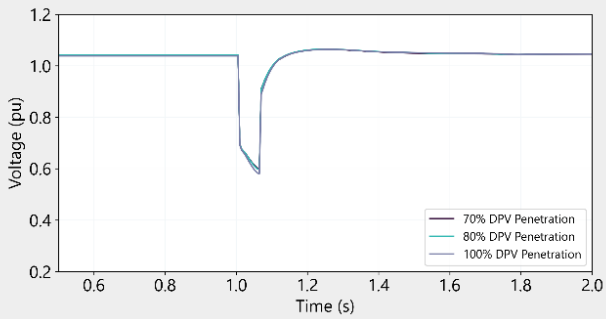
27<sup>th</sup> March 2024 event (0.6pu at TIPS A)



27<sup>th</sup> March 2024 event with severe fault (0.2pu at TIPS A)



Positive Sequence Voltage



## 6 Summary and recommendations

### 6.1 Summary of findings

Validation against measurements from these three events demonstrates that the CMLD+DPV models consistently and significantly outperform ZIP-based models in representing both transient and steady-state conditions.

In almost all cases, the CMLD+DPV models provide an improved (and in many cases a significantly improved) representation of distributed PV and composite load as measured in these disturbances, compared with the traditional ZIP modelling approach.

#### 6.1.1 Shake-off behaviours

The models provide a reasonable indication of the shake-off behaviours observed from distributed PV and composite load in response to deep voltage disturbances, which cannot be replicated at all by the traditional ZIP modelling approach. Figure 44 summarises the observed DPV and load shake-off in these three disturbances (“Target value”), compared with the CMLD and DPV model outcomes:

- The DPV model captures DPV shake-off reasonably accurately in all three cases.
- The CMLD model demonstrates a very considerable amount of load shake-off in the Victorian disturbance but underestimates the full extent of what was observed. The CMLD model overestimates load shake-off in both the South Australian disturbances. This highlights the need for uncertainty margins when applying these models.

Both models provide a considerable improvement over the traditional ZIP model, which does not represent any shake-off at all.

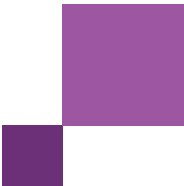
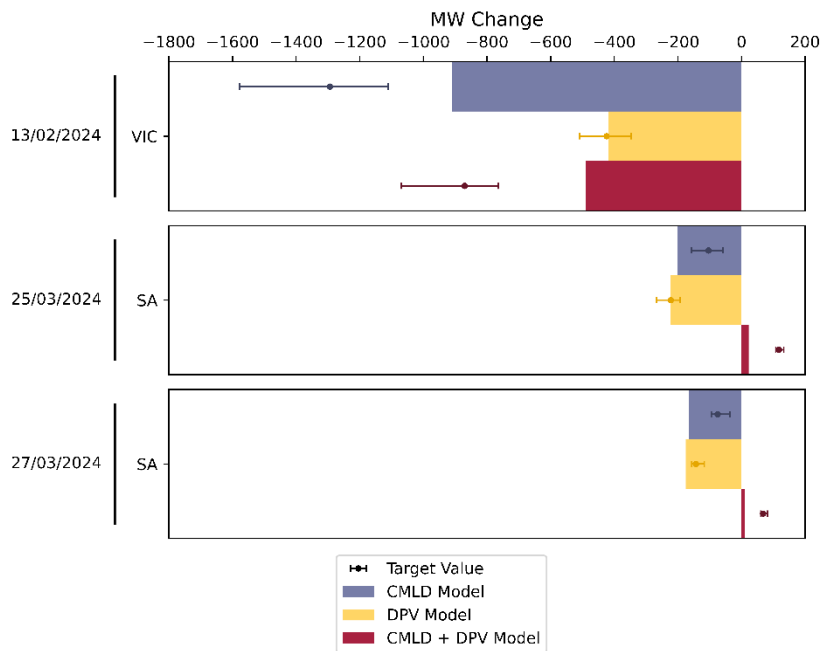


**Figure 44 CMLD & DPV model performance across three disturbances**



### 6.1.2 Transient behaviours

The models also provide a much-improved representation of the transient behaviours of composite load and distributed PV, especially for reactive power.

Importantly, the CMLD+DPV models accurately capture the transient “swing” in operational demand that occurs in cases with a high level of DPV operating. This behaviour is observed at radial load feeders supplied by a high proportion of DPV and is replicated well by the CMLD+DPV models. The composite load (CMLD) recovers post fault slightly faster than the distributed PV, leading to a significant transient deficit in generation that is much larger than the settling difference related to DPV and load shake-off. This can lead to a significant transient (~200ms duration) increase in regional operational demand post fault (for example, in South Australia the swing magnitude can exceed ~1000 MW in some projected cases with high levels of DPV operating). From a frequency control perspective, a 1 GW abrupt increase in demand is equivalent to losing a large generator and it could lead to a momentary dip in system frequency if not countered quickly.

These effects can have significant impacts on modelling outcomes and power system stability. This highlights the importance of applying accurate models for composite load and distributed PV, particularly in cases with a significant amount of DPV operating.

There is also a risk that protective relay systems (for example, rate-of-change-of-frequency or low-voltage load shedding relays) might respond unpredictably to such a rapid fluctuation. While the system maintained stability in the studied events, these findings highlight the potential need for additional damping and fast-acting controls when DPV penetration is high. In particular, system operators may consider deploying Fast Frequency Response (FFR) resources or other rapid reserve mechanisms to cushion the impact of these swings. Strengthening inertial support and tuning governor/ Automatic Governor Controller (AGC) settings for faster response could also help manage the 200 ms, 1000 MW spikes so that frequency remains within acceptable bounds and no spurious

protection trips occur. As DPV related demand swings grow in scale, the power system may require enhanced stability tools to maintain secure operation through the immediate aftermath of faults.

### 6.1.3 Limitations of the CMLD+DPV models

While the CMLD+DPV models represent a considerable improvement compared with the traditional ZIP model representation, these models have some important limitations. TNSPs and other users should be aware of these limitations, and carefully consider if the models are fit for purpose for the specific application.

Limitations include:

- **±30% Shake-Off Uncertainty:** The models exhibit uncertainty margins of  $\pm 30\%$  of the contingency size in capturing DPV and load shake-off.
- **Multiple faults:** The models only represent the shake-off associated with the first fault, and then “lock out” any subsequent shake-off that may occur in response to subsequent (potentially deeper) faults. This means it’s important for multi-fault events that the first fault modelled is the most severe (otherwise the models will under-represent the total amount of shake-off).
- **Importance of using both models together:** The studies emphasise the importance of using the CMLD model together with the DPV model. If only the DPV model is used (in conjunction with the traditional ZIP model), the load shake-off will not be captured and the model outcomes can be severely incorrect in some cases.

## 6.2 Recommendations

AEMO provides the following recommendations:

- **Review of Limit Advice:** TNSPs are urged to revisit their limit advice, ensuring it appropriately accounts for the dynamic behaviours of load and DPV observed during disturbances. Impacts to limits could be related to DPV and load shake-off, and to the significant transient “swing” in operational demand that is observed post fault and can be much larger than the settling shake-off levels. The studies presented in this report indicate that the CMLD+DPV model provides a considerable improvement compared with the traditional ZIP model, and that these models can lead to some important behaviours that may significantly impact power system stability and security limits. TNSPs retain responsibility for ensuring the models used for any studies are fit-for-purpose. In some cases, it may remain appropriate to continue application of simpler ZIP modelling approaches (or other load/DPV models).
- **Model Applicability:** Any use of these models must account for their known limitations, and their validity should be confirmed for each specific application. AEMO will continue collaborating with TNSPs to refine and validate the models, especially as they are applied to novel use cases.
- **Data Requirements:** These studies highlight the need for AEMO to collaborate with stakeholders to improve datasets for assessing power system behaviours and validation of power system models. This includes:
  - **High-Speed Monitoring:** High speed monitoring is required at a much wider range of radial load locations to monitor high-resolution data across different load compositions (residential, commercial, and industrial), DPV penetration levels (low and high), and voltage levels (transmission, sub-transmission, and

distribution). The rollout of PMUs across the network in progress at present should deliver a considerable improvement that will assist these efforts.

- **DPV fleet data:** Interval data is required from a diverse sample of individual DPV devices in the field to better estimate disconnection rates and quantify DPV behaviours during disturbances.
- **High speed inverter data:** High-speed data from various DPV inverter manufacturers with significant market shares in the NEM is needed to refine the understanding of DPV transient behaviours. This could include measurements via bench testing of inverters in the laboratory, and/or high-speed field measurements from a suitable sample of individual inverters.
- **Aggregate Load Composition:** Expand information on the composition of aggregate loads across the NEM to improve the representation of load dynamics in the models.

These actions will help refine model accuracy, increase confidence in the validity of the models, and enhance AEMO’s ability to plan and operate the power system securely in the context of increasing DPV penetration and evolving network dynamics.

### 6.3 Future improvements

There remain many areas where there is a need for continuing improvement of DPV and composite load models. Some known areas are outlined in Table 17.

**Table 17 Known model limitations and areas for improvement**

Limitation	Description
<b>DPV &amp; load shake-off uncertainty: ±30%</b>	<p><b>Limitation:</b> The CMLD and DERAEMO1 models provide the best available estimates for DPV and load shake-off behaviours during disturbances. However, they demonstrate uncertainty margins of ±30%. This variability arises from inherent challenges in accurately representing distributed PV generation behaviour and load dynamics during faults.</p> <p><b>Why Improvement is Needed:</b> Reducing this uncertainty would enhance the reliability of operational planning and limit advice. Improved accuracy would enable more precise assessments of system stability and reduce the need for conservative operating margins.</p>
<b>Transient behaviours</b>	<p><b>Limitation:</b> The models accurately represent the trajectory of active and reactive power flows during faults but tend to underestimate peak active power flows and overestimate peak reactive power flows. These discrepancies are particularly noticeable during transient conditions.</p> <p><b>Why Improvement is Needed:</b> Transient behaviours play a critical role in system protection and stability. Accurately modelling these responses is essential to understanding the dynamic impact of load and distributed PV on the NEM. Refining transient performance would also further enhance confidence in the models for dynamic studies.</p>
<b>Multiple faults</b>	<p><b>Limitation:</b> When multiple faults occur in close succession, the DPV and CMLD models only represent the shake-off behaviour based on the depth of the first fault. Multiple faults are likely to cause additional shake-off, but this is not captured by the models. Additionally, subsequent voltage disturbances often result in larger reactive power magnitudes than observed at PMU locations.</p> <p><b>Why Improvement is Needed:</b> Enhancing the models to account for multiple faults would provide more realistic simulations of these complex cases.</p>
<b>Distributed Battery Energy Storage (BESS) model</b>	<p><b>Limitation:</b> The current DERAEMO1 model is calibrated to represent DPV but has not been extended to include other types of Distributed Energy Resources such as BESS. Australian BESS installations are forecast to reach 5.6 GW by 2036–37<sup>30</sup>.</p>

<sup>30</sup> AEMO (May 2021) Behaviour of distributed resources during power system disturbances, <https://aemo.com.au/-/media/files/initiatives/der/2021/capstone-report.pdf>.

Limitation	Description
	<p><b>Why Improvement is Needed:</b> As BESS adoption grows, it will become a key component of the power system.</p>
Electric Vehicle (EV) model	<p><b>Limitation:</b> AEMO projects that by 2034, 4 million EVs (25% of passenger vehicles) will require grid charging<sup>31</sup>. However, there is currently no load model in PSS/E that simulates the dynamic and steady-state behaviours of EVs, particularly under fault conditions.</p> <p><b>Why Improvement is Needed:</b> EVs introduce unique challenges to the grid, including increased load variability and potential impacts on fault currents.</p>
Variable frequency drive (VFD) motor model	<p><b>Limitation:</b> While WECC has developed a positive sequence VFD motor model for integration into the CMLD architecture<sup>32</sup>, current implementations treat VFDs as algebraic power electronic loads. This approach fails to capture the full transient behaviour of VFDs.</p> <p><b>Why Improvement is Needed:</b> VFDs are increasingly common in industrial and commercial settings.</p>
Data centres	<p><b>Limitation:</b> Current load models do not explicitly account for the unique energy consumption patterns and dynamic behaviours of data centres. These facilities typically operate with high and stable loads but exhibit distinct power quality requirements, backup generation responses, and cooling system interactions during grid disturbances. With data centre energy demand rapidly increasing, driven by cloud computing, AI, and digital infrastructure needs, this gap poses a significant challenge. For instance, data centres already account for 23% of Virginia’s total power consumption<sup>33</sup>, and AEMO has suggested that existing and committed data centres are forecast to make up over 5% of the total large industrial load by 2033-34<sup>34</sup>.</p> <p><b>Why Improvement is Needed:</b> Data centres are becoming one of the largest energy consumers globally and are expected to place growing demands on the grid. Accurate modelling of their demand-response behaviours, and reliance on uninterruptible power supplies (UPS) during faults is essential to predict their impact on grid stability. Specialised data centre models or the improvement of existing CMLD models would enable better grid integration and planning, particularly in regions with high data centre penetration such as New South Wales and Victoria<sup>35</sup>.</p>

<sup>31</sup> AEMO (August 2024), Electricity Statement of Opportunities (ESOO), [https://wa.aemo.com.au/-/media/files/electricity/nem/planning\\_and\\_forecasting/nem\\_esoo/2024/2024-electricity-statement-of-opportunities.pdf?la=en&hash=2B6B6AB803D0C5F626A90CF0D60F6374](https://wa.aemo.com.au/-/media/files/electricity/nem/planning_and_forecasting/nem_esoo/2024/2024-electricity-statement-of-opportunities.pdf?la=en&hash=2B6B6AB803D0C5F626A90CF0D60F6374)

<sup>32</sup> D. Ramasubramanian, P. Mitra and A. Gaikwad. 2018. VFD Model Development, <https://www.wecc.biz/Administrative/VFD%20Modeling-%20Ramasubramanian.pdf>.

<sup>33</sup> <https://www.epri.com/research/products/000000003002028905>

<sup>34</sup> AEMO (August 2024), Electricity Statement of Opportunities (ESOO), pg 34.

<sup>35</sup> AEMO (August 2024), Electricity Statement of Opportunities (ESOO), pg 27.

# A1. Glossary

Acronym	Details
<b>ASEFS2</b>	Australian Solar Energy Forecasting System 2: Designed to produce solar generation forecasts for large solar power stations and small-scale distributed photovoltaic (PV) systems up to 100 kW, covering forecasting timeframes from 5 minutes to 2 years.
<b>BESS</b>	Distributed Battery Energy Sources i.e. Tesla Powerwall units
<b>CB</b>	Circuit Breaker
<b>CER</b>	Clean Energy Regulator
<b>CMLD</b>	Composite Load Model
<b>CT</b>	Current Transformer
<b>DER</b>	Distributed Energy Resources
<b>DERAEMO1</b>	DERAEMO1: refers to AEMO's Distributed Energy Resource aggregate model used in PSS®E studies.
<b>DPV</b>	Distributed PV: this is the term used for rooftop PV and PV Non-Scheduled Generators combined.
<b>EV</b>	Electric Vehicles
<b>HSM</b>	High Speed Monitors
<b>HV</b>	Overvoltage (multiplier) with respect to the block diagram associated with the high voltage trip logic of the DPV model.
<b>LGC</b>	Large-scale Generation Certificates
<b>LRET</b>	Large-scale Renewable Energy Target: Large-scale Renewable Energy Target. A target scheme that incentivises the development of renewable energy power stations in Australia.
<b>MW</b>	Megawatts
<b>NEM</b>	National Electricity Market
<b>NER</b>	National Electricity Rules
<b>OD</b>	Operational Demand
<b>OEM</b>	Original Equipment Manufacturer
<b>PMU</b>	Phasor Measurement Unit: PMUs are high-speed sensors that measure voltage and current synchrophasors of the power system with the accuracy in the order of one microsecond using a common time source for synchronisation. They are high speed measurement devices.
<b>PARA</b>	Parafield Gardens
<b>PS</b>	Power Station
<b>PVNSG</b>	Photovoltaic Non-scheduled generation (100kW to 30 MW)
<b>SA</b>	South Australia
<b>SCADA</b>	Supervisory Control and Data Acquisition
<b>SLIB</b>	Single Load Infinite Bus
<b>SRES</b>	Small-scale Renewable Energy Scheme
<b>TNSP</b>	Transmission Network Service Provider
<b>UV</b>	Undervoltage (multiplier) with respect to the block diagram associated with the low voltage trip logic of the DPV model.
<b>VFD</b>	Variable Frequency Drives
<b>VIC</b>	Victoria

## A2. Data sources

The data sources used to estimate the behaviour of DPV and load during these incidents are summarised in the Table below.

**Table 18** Data sources used in this report

Category	Sources / types	Notes
High speed measurements	Voltages, active power, and reactive power measurements at key network nodes	Collected from high-speed monitoring at locations where available. Typically, 20ms resolution. PMU (Phasor Measurement Unit) data used where available.
	Radial loads	High speed measurements of radial loads are particularly important for validation of dynamic models because they provide insight into the dynamic behaviours of load and DPV with minimal complicating factors from the surrounding network and other generators. There is limited monitoring of radial loads at present, but further planned with the rollout of PMUs across the network.
Generation from DPV at the time of the incident	ASEFS2	The Australian Energy Solar Forecasting System 2 (ASEFS2) <sup>36</sup> produces aggregated regional solar generation forecasts for small-scale PV systems (<100kW). The capacity factors produced by ASEFS2 were also applied to the PV non-scheduled generation (PVNSG) fleet (assumed to be exposed to similar solar insolation levels).
Change in DPV in response to the incident	Solar Analytics	The change in DPV in response to the incident was estimated based on datasets provided by Solar Analytics <sup>37</sup> . Solar Analytics monitors a sample of thousands of individual DPV systems in the NEM at ~60s resolution. These individual DPV time series were analysed to identify systems that show active power drop in the interval immediately following the disturbance to estimate disconnection rates across the fleet. Disconnection rates were scaled up accounting for the fleet composition in different categories by inverter standard, size, and original equipment manufacturer (OEM) where sample sizes were large enough.
Load	Operational demand	Total operational demand (net of DPV) for the region was estimated from SCADA. SCADA measurements (typically 4s resolution) are summed from the terminals of generators in the region and interconnector flows. Since these are not time-synchronised, accuracy is limited for short time intervals (<30s). However, these measurements give a reasonable indication of changes in total load in the region where it is sustained over periods of longer than ~30s, such as load shake-off.
	Underlying demand	Underlying demand is estimated based on operational demand (from SCADA), plus the estimate of small-scale PV systems from ASEFS2, plus the estimate of PVNSG generation.
Installed capacity of DPV	Clean Energy Regulator (CER)	The CER collects data on installations of DPV under the SRES (Small-scale renewable energy scheme). This data was used to estimate the size of the DPV fleet installed at the date of the incident.
	PVNSG (PV non-scheduled generation)	The installed capacity of PVNSG (100kW to 30 MW) was estimated based on data collected by the CER under the Large-scale Renewable Energy Target (LRET) scheme. The LRET tracks historical Large-scale Generation Certificates (LGCs) in the REC registry as well as capacity of accredited projects and power stations. The DERAEMO1 model has been used to represent both rooftop PVs and PVNSG, with the assumption that they produce identical disturbance responses.
Composition of the DPV fleet	CER	There are different 'vintages' of DPV installed under different standards, which will change their dynamic behaviour in response to a power system incident. The CER

<sup>36</sup> AEMO, Australian Solar Energy Forecasting System, <https://aemo.com.au/en/energy-systems/electricity/national-electricity-market-nem/nem-forecasting-and-planning/operational-forecasting/solar-and-wind-energy-forecasting/australian-solar-energy-forecasting-system>

<sup>37</sup> For further information on these datasets and methodologies, refer to: AEMO (May 2021) Behaviour of distributed resources during power system disturbances, <https://aemo.com.au/-/media/files/initiatives/der/2021/capstone-report.pdf?la=en&hash=BF184AC51804652E268B3117EC12327A>

Category	Sources / types	Notes
		<p>datasets were used to split the composition of the fleet at the time of each disturbance into the following components, to inform model parameters:</p> <ul style="list-style-type: none"> <li>• % installed under AS/NZS4777.2:2020 – Installations from April 2023 to the time of the incident<sup>38</sup></li> <li>• % installed under AS/NZS4777.2:2015 – Installations between October 2016 to April 2023.</li> <li>• % installed under AS/NZS4777.2:2005 – Installations prior to October 2016.</li> </ul>

<sup>38</sup> Based on assessment of DPV compliance with standards, as documented in this report: Figure 15, AEMO (Dec 2023) Compliance of Distributed Energy Resources with Technical Settings: Update, [https://aemo.com.au/-/media/files/initiatives/der/2023/oem\\_compliance\\_report\\_2023.pdf?la=en&hash=E6BEA93263DE58C64FCC957405808CA6](https://aemo.com.au/-/media/files/initiatives/der/2023/oem_compliance_report_2023.pdf?la=en&hash=E6BEA93263DE58C64FCC957405808CA6)